END
DATE
FILMED

8-80

DTIC

ARACOR

AFOSR-TR- 80-0467

③

ADA086494

LEVEL

A STUDY OF LOW-TEMPERATURE PROCESSES IN
NON-EQUILIBRIUM ELECTRONIC STATES

FINAL REPORT
APRIL 1980

DTIC
ELECTE
JUL 7 1980
S
C
D

PREPARED FOR:

DIRECTOR OF PHYSICS
AIR FORCE OFFICE OF SCIENTIFIC RESEARCH
BUILDING 410
BOLLING AIR FORCE BASE, D.C.   20332

DDC FILE COPY

ADVANCED RESEARCH AND APPLICATIONS CORPORATION

80 7 2 10

ARACOR

A STUDY OF LOW-TEMPERATURE PROCESSES IN
NON-EQUILIRIUM ELECTRONIC STATES

Final Report
April 1980

By

T. C. Wang, T. J. Magee,
J. Peng and R. A. Armistead

Prepared for:

Director of Physics
Air Force Office of. Scientific Research
Building 410
Bolling Air Force Base, D.C.   20332

ADVANCED RESEARCH AND APPLICATIONS CORPORATION

1223 E. Arques Avenue, Sunnyvale, California 94086 (408) 733-7780

REPORT DOCUMENTATION PAGE	READ INSTRUCTIONS BEFORE COMPLETING FORM

1. REPORT NUMBER AFOSR-TR-80-0467	2. GOVT ACCESSION NO. AD-A086499	3. RECIPIENT'S CATALOG NUMBER

4. TITLE (and Subtitle) A STUDY OF LOW-TEMPERATURE PROCESSES IN NON-EQUILIBRIUM ELECTRONIC STATES.	5. TYPE OF REPORT & PERIOD COVERED Final Report. Feb 78 - Jan 80
	6. PERFORMING ORG. REPORT NUMBER

7. AUTHOR(s) T. C. Wang, T. J. Magee, J. Peng, and R. A. Armistead	8. CONTRACT OR GRANT NUMBER(s) F49620-78-C-0010

9. PERFORMING ORGANIZATION NAME AND ADDRESS Advanced Research & Applications Corporation 1223 East Arques Avenue Sunnyvale, CA 94086	10. PROGRAM ELEMENT, PROJECT, TASK AREA & WORK UNIT NUMBERS 61102F 2301/A5

11. CONTROLLING OFFICE NAME AND ADDRESS Air Force Office of Scientific Reserach (AFOSR) NP Bolling Air Force Base Washington, D.C. 20332	12. REPORT DATE April 1980
	13. NUMBER OF PAGES 56

14. MONITORING AGENCY NAME & ADDRESS(If different from Controlling Office)	15. SECURITY CLASS. (of this report) UNCLASSIFIED
	15a. DECLASSIFICATION/DOWNGRADING SCHEDULE

16. DISTRIBUTION STATEMENT (of this Report)

Approved for public release; distribution unlimited.

17. DISTRIBUTION STATEMENT (of the abstract entered in Block 20, If different from Report)

18. SUPPLEMENTARY NOTES

19. KEY WORDS (Continue on reverse side if necessary and identify by block number)

Josephson tunnel junction	Quasiparticles
Microbridges	Laser annealing
Superconductors	Grain size
Low temperature processes	Niobium films

20. ABSTRACT (Continue on reverse side if necessary and identify by block number)

Primary focus was directed to experimental studies of the electrical behavior of weakly-coupled superconductors. Two types of superconducting devices were used, Josephson tunnel junctions and superconducting thin-film microbridges. The experiments showed that non-equilibrium states created by microwave irradiation and quasiparticle injection will change the current -

DD FORM 1473
1 JAN 73

voltage characteristics of Josephson devices. Experiments were also conducted to determine if the grain size of superconducting niobium (Nb) films could be controlled using scanning laser annealing. Initial (as deposited) grain sizes were dependent upon the deposition technique. Regardless, laser annealing resulted in substantial modifications to the structure of the Nb films. With proper laser annealing techniques, relatively fine-grained polycrystalline films were converted to large polycrystalline grains with an average size of 5 µm x 10 µm.

→ 5 by 10 nanometers.

Accession For

A STUDY OF LOW-TEMPERATURE PROCESS IN
NON-EQUILIBRIUM ELECTRONIC STATES

I. INTRODUCTION

The general objective of this research program was to study non-equilibrium processes in thin superconducting Josephson junctions near 4°K. Non-equilibrium processes in superconductors have received renewed theoretical attention because of problems in high-frequency weak links. From the results of experiments performed in this program, it is hoped that a better basis will be provided for further understanding these phenomena. Improved theory could also provide a guide to increasing the sensitivity and frequency range of superconducting detectors, receivers, and mixer electronics which have important civilian and military applications. Ultimately, through the collective and integrated results of a large number of programs like this one, it is hoped that superconducting materials with increased transition temperatures may be developed.

The primary effort was directed to experimental studies of the electrical behavior of weakly-coupled superconductors. Two types of superconducting devices were employed in this program, Josephson tunnel junctions and superconducting thin-film microbridges. An initial part of the program, which was certainly non-trivial, was the design of a suitable experimental cryostat and the development of procedures for the fabrication of high-quality superconducting test devices.

The specific focus of the experiment was to further the understanding of electron pairing under the influence of high-frequency fields. The effect of high-frequency fields on superconductors is quite complicated and the role of non-equilibrium excitations generated by the field is very important. In fact, a time-dependent field tends to change the distribution function of quasiparticles in energy. This process will generate new excitations and shift them to higher energies.

On the other hand, there are always processes of energy relaxation due to the interaction of electrons with lattice oscillations (phonons) or with each other. These relaxation processes can result in a non-equilibrium stationary distribution of excitations. One important experimental manifestation of this phenomenon is the enhanced superconductivity that has been observed in the presence of a high-frequency field.

There are other methods that can be used to probe the non-equilibrium superconducting state, quasiparticle and/or the phonon injection. In this report, we will present some results on the tunneling characteristics of Josephson junctions in the presence of quasiparticle injection.

One can also explore the modification of electron coupling through phonon interaction by varying the electron mean free path. The effect of mean-free-path modification can be assessed through the study of granular superconducting films with varying grain sizes. Limited attention in this program was directed to a study of how to control superconducting film grain sizes and how to substantially increase the average grain size of a film. In addition to evaluating alternative film deposition methods for superconducting niobium (Nb) films, laser annealing experiments were conducted in the attempt to establish procedures, for controllably increasing the grain size of deposited films.

The next section, Section II, presents a background of the current state of the understanding of non-equilibrium superconductivity. Section III describes the experimental techniques and apparatus used in this study. This section also presents a discussion of experiments conducted with superconducting thin-film microbridges under the influence of high-frequency fields and on Josephson tunnel junctions in the presence of quasiparticle injection. The results of preliminary experiments using laser annealing to

alter the structure and grain size of Nb thin films prepared by different techniques are also reported. In Section IV, the overall results are discussed and related to problems that remain to be solved.

Appendix A provides a reprint of "Current-Density Distribution in Josephson Tunnel Junctions", which was based on the research conducted in this program and published in the Journal of Applied Physics. This part of the program was directed to the distribution and the peak amplitude of Fiske modes in Josephson junctions. The analysis showed that the peak value can vary over a large range, depending upon whether the junction is "good" or "bad" (in the sense of the uniformity of the oxidation barrier). Thus, it is suggested that a study of the field dependence of Fiske modes should reveal the uniformity of the oxidation barrier of a Josephson tunnel junction. However, it is observed that there is no unique current-density distribution that corresponds to a particular observed field dependence.

Appendix B provides a copy of, "Getting to the Competitive Market Place with Josephson Junction Devices", a paper presented at a conference on the "Future Trends in Superconducting Electronics.

II. BACKGROUND

II.1 Weakly-Coupled Superconductivity

The superconducting state can be modelled as a condensation
of electron states. When the temperature is below a certain criti-
cal temperature, Tc, the electrons, due to the electron-phonon-
electron interaction, tend to form so-called Cooper pairs. When
this occurs, the ground state of the superconductor[1] is separated
from the first excited state by a certain amount of energy - the
energy gap, Eg = 2Δ (A minimum energy of 2Δ is required to break a
pair of electrons). The electron pairs are condensed into the same
state and, using a simplified picture, the electron pairs all have
the same wavefunction, ψ (γ) (In Ginzburg-Landau theory, ψ (γ) is
just the order parameter), where γ is the position of the center of
mass of the pair.

If we let p (γ) be the local density of electron pairs, the
wavefunction can be written as $\psi(\gamma) = \sqrt{\rho(\gamma)}e^{i\theta}$. The phase, θ, is
a quantity possessing long-range order. That is, if we know its
value at one point inside the superconductor, we can determine its
value at any other point.

When two superconductors are separated by a very thin insulating
barrier or a constricted region (See Figure 1), the phase coherence
can extend from one superconductor to the other. This will permit
electron pairs to flow between them, even at zero voltage. Current,
up to a certain value, can exist before a finite voltage appears.
The supercurrent in such a weakly-coupled superconducting system is
described by the famous Josephson equation[2]

$$Js = Jo \sin \phi \qquad\qquad\qquad (1)$$

4
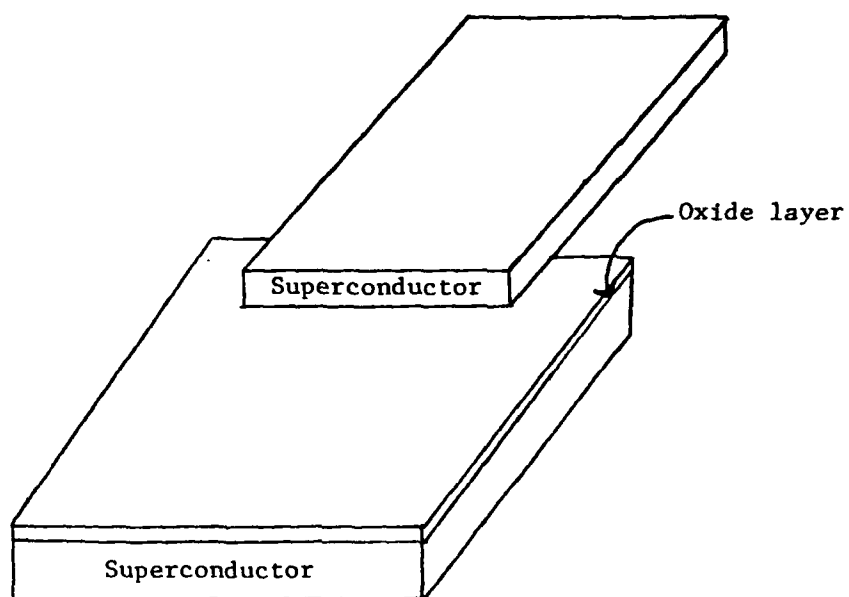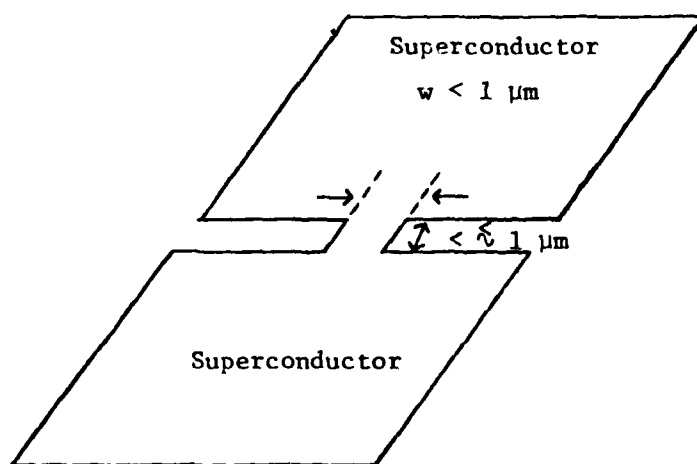
a) Tunnel Junction

b) Thin-Film Microbridge

Figure 1. Schematic of Josephson Tunnel Junction
and Microbridge Structures

5

where, Js is the supercurrent density, Jo is the critical current
per unit area, and ϕ is the change in the phase from one supercon-
ductor to the other. This phase-dependent supercurrent is the
most important parameter in determining the microscopic properties
of a junction.

Besides the supercurrent, there can be tunneling of quasi-
particles; these are excitations in the superconductors, with
properties like ordinary electrons. At zero voltage, there is an
equal probability of quasiparticle tunneling from either side of
the barrier to the other, so there is no net quasiparticle current.
When there is a finite voltage across the barrier, a net quasipar-
ticle current appears. A characteristics curve of a Josephson
junction, including both the supercurrent and quasiparticle tunnel-
ing, is shown in Figure 2. The sudden increase of the quasiparticle
current at a voltage equal to the energy gap, is due to the paired
electrons breaking process, as mentioned before.

In the presence of a DC voltage, the Josephson supercurrent
will oscillate with a frequency proportional to the factor 2e/h =
483 GHz/mV. The time-dependent phase difference is described by
the equation,[2]

$$\frac{\partial \phi}{\partial t} = \frac{2eV}{h} \tag{2}$$

where, e is the electron charge, h is the Planck constant divided
by 2π, V is the voltage.

If there is a high-frequency field in addition to the DC vol-
tage, then the total voltage across the junction will be $V = V_{ac} +$
$V_{rf} \sin wt$. In this equation, V_{rf} describes the amplitude of the
high-frequency field and w is the frequency. Combining equation (1)
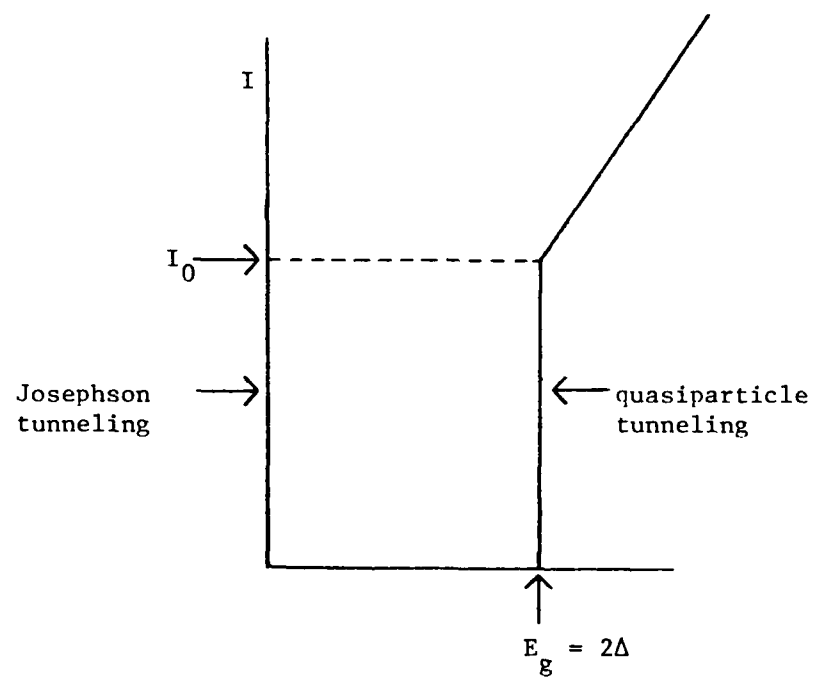and (2), it can be easily shown that the junction will convert those

6

Figure 2. Josephson Junction Characteristic Curve

high-frequency signals into a DC current at $V_{dc}=h\omega/2e$. This forms the basis of a high-frequency Josephson junction detector. On the other hand, if the junction is biased at Vdc, it will radiate a high-frequency signal at $\omega=2eV_{dc}/h$. If a large array of Josephson junctions can be made to radiate coherently, it could be used as an extremely-high-frequency microwave source.

II.2 Superconducting Non-equilibrium States

An introductory description of the superconducting non-equilibrium states is given in the referenced proposal[3]. The general features of the non-equilibrium state is that due to the perturbation of a high-frequency field or quasiparticle injection, the excitation spectrum of a superconductor will change. Those quasiparticles that gain energy will go through a certain sequence of relaxation processes; some of them will form excess pairs and some of them will lose energy via inelastic scattering. If the perturbation is shorter than a certain characteristic time, both quasiparticle recombination and pair electron relaxation processes will be measurable. If the perturbation is long enough, the system will be driven into a new non-equilibrium stationary state; in this case, the energy gap and the Josephson supercurrent are the relevant measurable quantities.

Eliasberg[4-7] has developed a theory for such a stationary non-equilibrium system. Based on the microscopic theory of superconductivity (BCS theory), the equation of the gap is written as,

$$1 = \tau \int_{\Delta}^{\infty} \frac{d\epsilon}{\sqrt{\epsilon^2 - \Delta^2}} \{1 - \eta\epsilon\} \tag{3}$$

where, τ is the BCS interaction parameter (it is a direct measure of the pairing strength), Δ is the energy gap parameter, and ϵ is the energy of the quasiparticles. $\epsilon = \sqrt{\Delta^2 + E_k^2}$, E_k is the kinetic energy of the quasiparticle measured from the Fermi level.

8

In the non-equilibrium state, the Fermi function, $\eta(E) = \{e^{E/kT} + 1\}^{-1}$ has to be replaced by a new distribution function. Eliasberg used the perturbation method and wrote $\eta(\varepsilon) = \eta_0(\varepsilon) + \eta_1(\varepsilon)$, with $\eta_0(\varepsilon)$ denoting the Fermi function and $\eta_1(\varepsilon)$ a small deviation. Using this form, he was able to solve for $\eta_1(\varepsilon)$ and get an expression for $\eta_1(\varepsilon)$ as a function of microwave power.

Eliasberg's analysis includes absorption, spontaneous emission and pair breaking processes. Unfortunately, the parameter for the applied microwave power, $\alpha = 1/3 \, v_F \ell \, e^2 A\omega^2 / \hbar c^2$, ($v_F$ is the Fermi velocity, ℓ is the mean free path for elastic scattering, $A\omega$ is the amplitude of the microwave field, e is the electron charge, c is the speed of light, and $\hbar$ is the Planck constant divided by 2π), is not an easily measurable quantity.

In the theory of transient processes of nonequilibrium super-conductors developed by Stoeckly,[8] the driving strength parameter of the microwave perturbation is written as

$$A_{microwave} = \frac{2\tau_o R_N H^2}{dN(o)\omega^2} \left(\frac{Tc}{\Delta o}\right)^3, \qquad \text{where } \tau_o \text{ is the normal state}$$

electron scattering time, H is the magnetic field of the microwave photons, R_N is the normal state surface resistance, N(o) is the single spin density of state at the Fermi energy in the normal state, d is the film thickness, ω is the microwave frequency, Tc is the critical temperature and Δo is the gap parameter at zero temperature.

It is because of the difficulties of measuring these micro-wave parameters precisely that makes a meaningful comparison of experimental results with theory a major challenge and a contin-uing problem.

However, the Eliasberg and the Stoeckly theories give either a formula or a numerical solution of the energy gap parameter. Thus, a comparison with experiments is possible. In Eliasberg's solution, a comparison of theory with experiment will require the

9

measurement to be done at temperatures very close to Tc. In Stoeckly's theory, a short microwave pulse will be required. A discussion about the test of Stoeckly's theory is provided elsewhere[3].

In Section III, we will present some results of the non-equilibrium states in microwave-perturbed superconducting micro-bridges and quasiparticle-injected Josephson tunnel junctions.

III. EXPERIMENTAL

The standard four-point probe method was used to character-
ize the DC current-voltage characteristics of the devices (see
Figure 3). Four gold contacts were deposited before adding the
bottom layer of film. Two of the terminals were used for the cur-
rent and two for the voltage measurement. The junctions, after
fabrication, were stored in liquid nitrogen until the measure-
ments were made.

Two types of Josephson junctions were fabricated, one was
tin-tin oxide-tin and the second type was a multi-layer lead-tin-
tin oxide-tin-lead junction. In the case of the tin-tin oxide-tin
junction, the tin films were around $1400\overset{o}{A}$ thick; the separate
layer thicknesses of the lead-tin-tin oxide-tin-lead junctions
were as follows: lead film, $1200\overset{o}{A}$ and tin film, $200\overset{o}{A}$. The sub-
strate temperature was maintained at $-50^{o}C$ during deposition.

The submicron thin-film microbridges were fabricated using
electron-beam lithographic techniques using indium as the bridge
material. A flow chart of the fabrication is described in Figure
4.

The nominal thickness of the indium film was $1000\overset{o}{A}$ and the
substrate was maintained at liquid nitrogen temperature during
deposition. Extra care had to be taken during the wire bonding,
handling and testing of the thin-film microbridges, because they
are more sensitive to burnout than tunnel junctions. This is
because heat dissipation in tunnel junctions is three dimensional,
while in the case of the submicron microbridges, it is only two
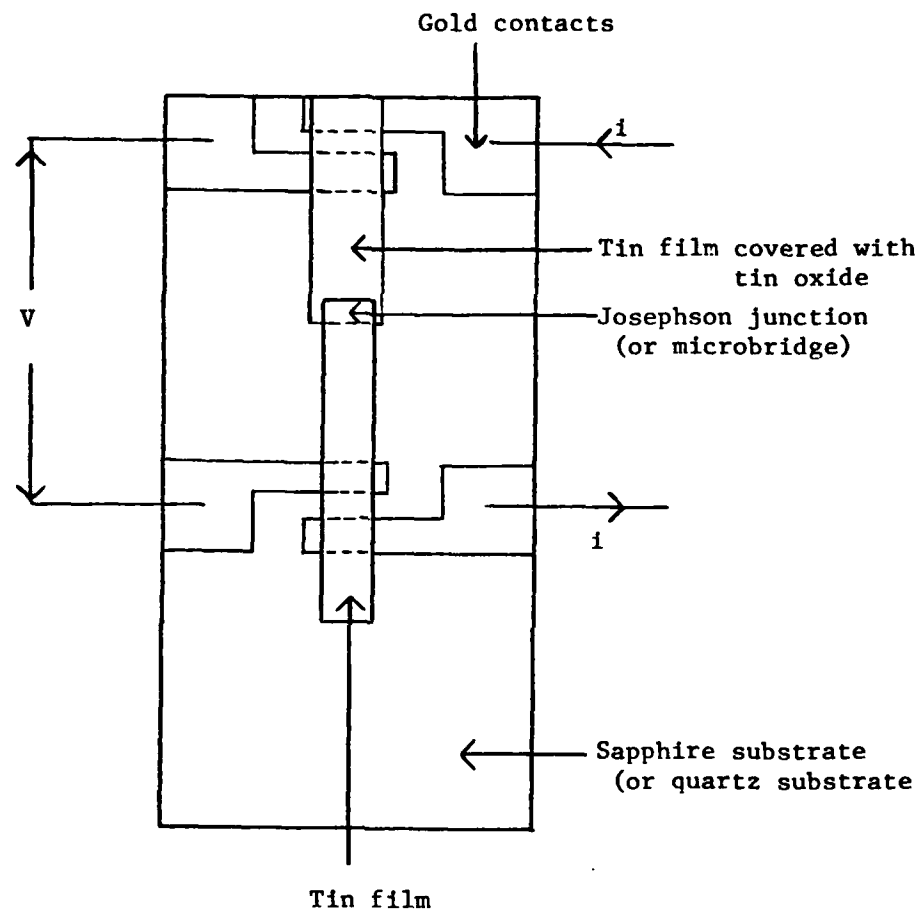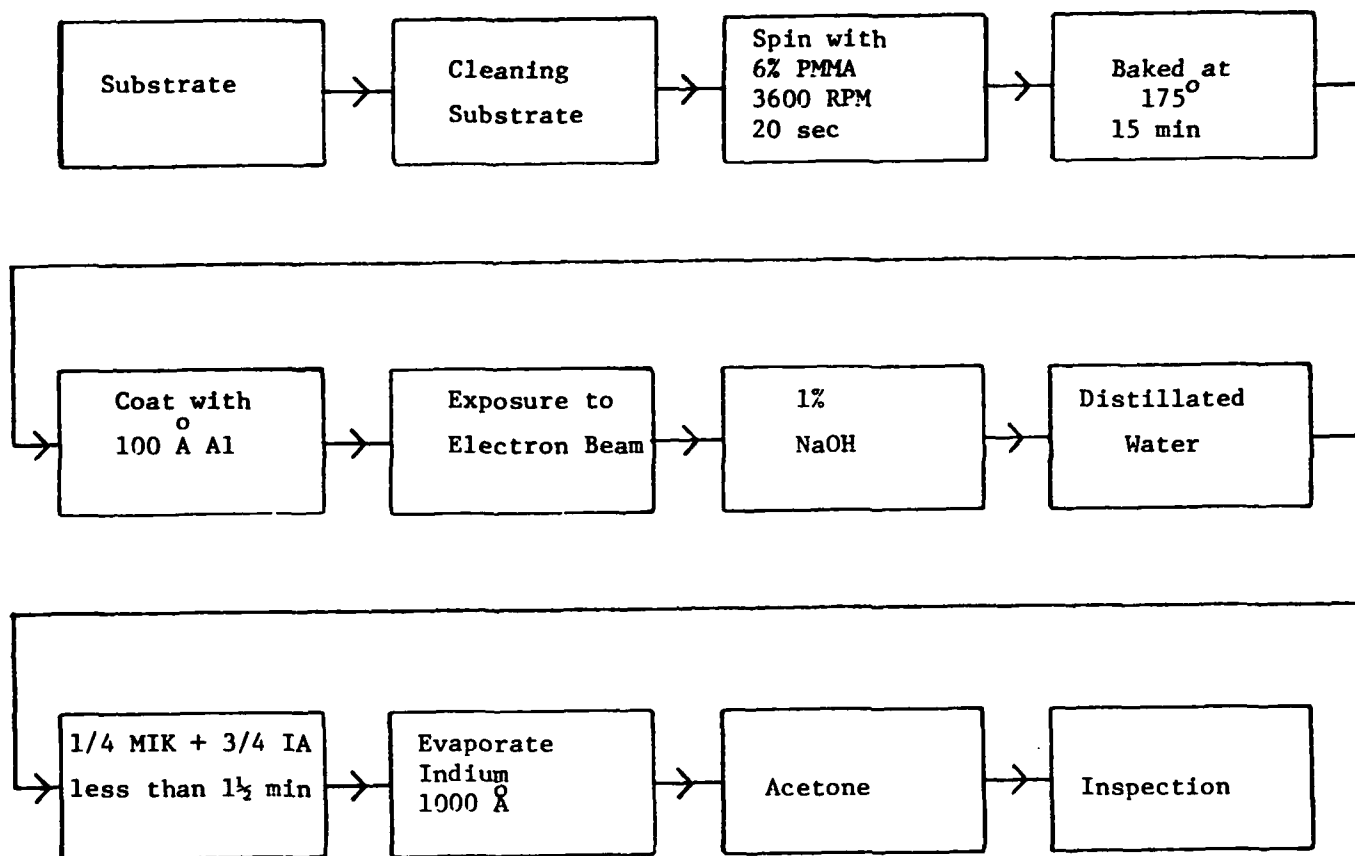dimensional.

11

Figure 3. Configuration of Test Structures to
Enable Four-Point Probe Measurements

12

```
┌─────────────┐     ┌─────────────┐     ┌─────────────┐     ┌─────────────┐
│             │     │             │     │ Spin with   │     │             │
│  Substrate  │ ──▶ │  Cleaning   │ ──▶ │ 6% PMMA     │ ──▶ │ Baked at    │
│             │     │  Substrate  │     │ 3600 RPM    │     │   175°      │──┐
│             │     │             │     │ 20 sec      │     │ 15 min      │  │
└─────────────┘     └─────────────┘     └─────────────┘     └─────────────┘  │
  ┌──────────────────────────────────────────────────────────────────────────┘
  │
  │ ┌─────────────┐     ┌─────────────┐     ┌─────────────┐     ┌─────────────┐
  │ │ Coat with   │     │             │     │             │     │             │
  └▶│     °       │ ──▶ │ Exposure to │ ──▶ │    1%       │ ──▶ │ Distillated │──┐
    │ 100 A Al    │     │Electron Beam│     │   NaOH      │     │   Water     │  │
    │             │     │             │     │             │     │             │  │
    └─────────────┘     └─────────────┘     └─────────────┘     └─────────────┘  │
  ┌──────────────────────────────────────────────────────────────────────────────┘
  │
  │ ┌─────────────┐     ┌─────────────┐     ┌─────────────┐     ┌─────────────┐
  │ │1/4 MIK + 3/4 IA│  │ Evaporate   │     │             │     │             │
  └▶│less than 1½ min│─▶│ Indium      │ ──▶ │  Acetone    │ ──▶ │ Inspection  │
    │             │     │ 1000 Å      │     │             │     │             │
    └─────────────┘     └─────────────┘     └─────────────┘     └─────────────┘
```

Note:

        PMMA is polymethyl methacrylate electron resist
        MIK is methyl isobutyl ketone
        IA is isopropanol alcohol

        Figure 4. Flow Chart of the Fabrication Process for Microbridges

During the measurement, the devices were immersed directly in liquid helium in an insulated non-magnetic dewar. The sample region was magnetically shielded by a high-permeability metal can.

The temperature was measured using a germanium resistor calibrated against the liquid helium vapor pressure; accuracies to about $5m^{o}K$ were achieved. A 100-ohm heater at the bottom of the device was used to stir the liquid helium to keep the temperature uniform.

The circuits were carefully shielded and all D.C. leads were separated from the samples with rf filters. The microwave signal was supplied through a coaxial cable, and the microwave power was read through an attenuator. A 9-GHz microwave source and a frequency doubler was used to provide an 18-GHz signal.

The current-voltage characteristics of a device was displayed on an oscilloscope or an X-Y recorder using an A.C. triangle-wave generator.

III.1 Electrical Behavior of Thin-Film Microbridges;

   D.C. Characteristics and A.C. Josephson Effect: The dimensions of the thin-film microbridges were typically smaller than 1 µm x 1 µm. Table 1 lists the dimensions of the microbridges studied in this program and indicates whether the A. C. Josephson effect was observed. These results clearly show that smaller bridges will be better for microwave applications.

A review of these data indicate that the briges that exhibit a well-defined A. C. Josephson effect usually have a very low resistance, i.e., less than 1 ohm. It is prehaps for this reason that thin-film microbridges have not been able to demonstrate the capability of being a low-noise extremely-sensitive high-frequency detector as have tunnel junctions.

14

Table 1

Sample No.	Microbridge Dimension (W x L) (micron)	Normal Resistance (ohm)	A.C. Josephson Effect
B1	0.65 x 0.72	0.30	Yes
B2	0.70 x 7.0	1.22	No
B3	0.48 x 0.50	0.22	Yes
B4	0.38 x 0.65	0.38	Yes
B5	0.28 x 0.75	0.43	Yes

Figure 5 shows typical current-voltage characteristics curves of a microbridge with and without microwave perturbation. The DC current steps appear at a voltage, $V_{dc} = \frac{n\hbar\omega}{2e}$; n, an integer, is the mode number. These steps correspond to synchronized oscillations between the rf signal and the A. C. Josephson current.

The sensitivity of a Josephson detector is critically dependent on its DC characteristics. In Figure 6, the power dependence of the Josephson supercurrent and the fundamental step is plotted. It is generally realized that if the commonly-accepted RSJ (Resistance-shunted junction) model[9,10] is used, the Josephson supercurrent shows a $J_0(V_{rf})$ (Bessel function of order 0) dependence, and the fundamental step shows a $J_1(V_{rf})$ (Bessel function of order 1) dependence. However, in the case of microbridges, such a dependence is not observed. Therefore, care must be taken in applying the RSJ model for predicting the high-frequency response of a microbridge.

III.1.1 Microwave-Irradiated Non-equilibrium States: An interesting observation that can be drawn from Figure 5 is that the Josephson supercurrent increases slightly, reaches a maximum, then decreases as the rf power increases further; this is common for small microbridges. This behavior is consistent with Eliasberg's theory of the non-equilibrium stationary states of superconductors. It is interesting to note that Eliasberg's theory suggests that it is possible to increase the superconducting transition temperature with the application of rf irradiation. Even though such an increase is not of a significant amount, it does suggest that a suitable external perturbation can be used to increase the superconducting transition temperature of a superconductor by changing the excitation spectrum.

III.1.2 Electrical Behavior of Josephson Tunnel Junction's DC
            Characteristics: A typical current-voltage characteristics curve of a tin-tin oxide-tin Josephson junction is shown in Figure 7. The supercurrent shows diffraction-pattern dependence on the externally-applied magnetic field, as it should. It

16

$T = 3.411^{\circ}K$ $L = 0.65~\mu m$

$\omega = 18$ GHz $W = 0.38~\mu m$

n=2

17dB   12dB   10dB   9dB   8dB   6dB

10 μV

n=1

I_{rf}
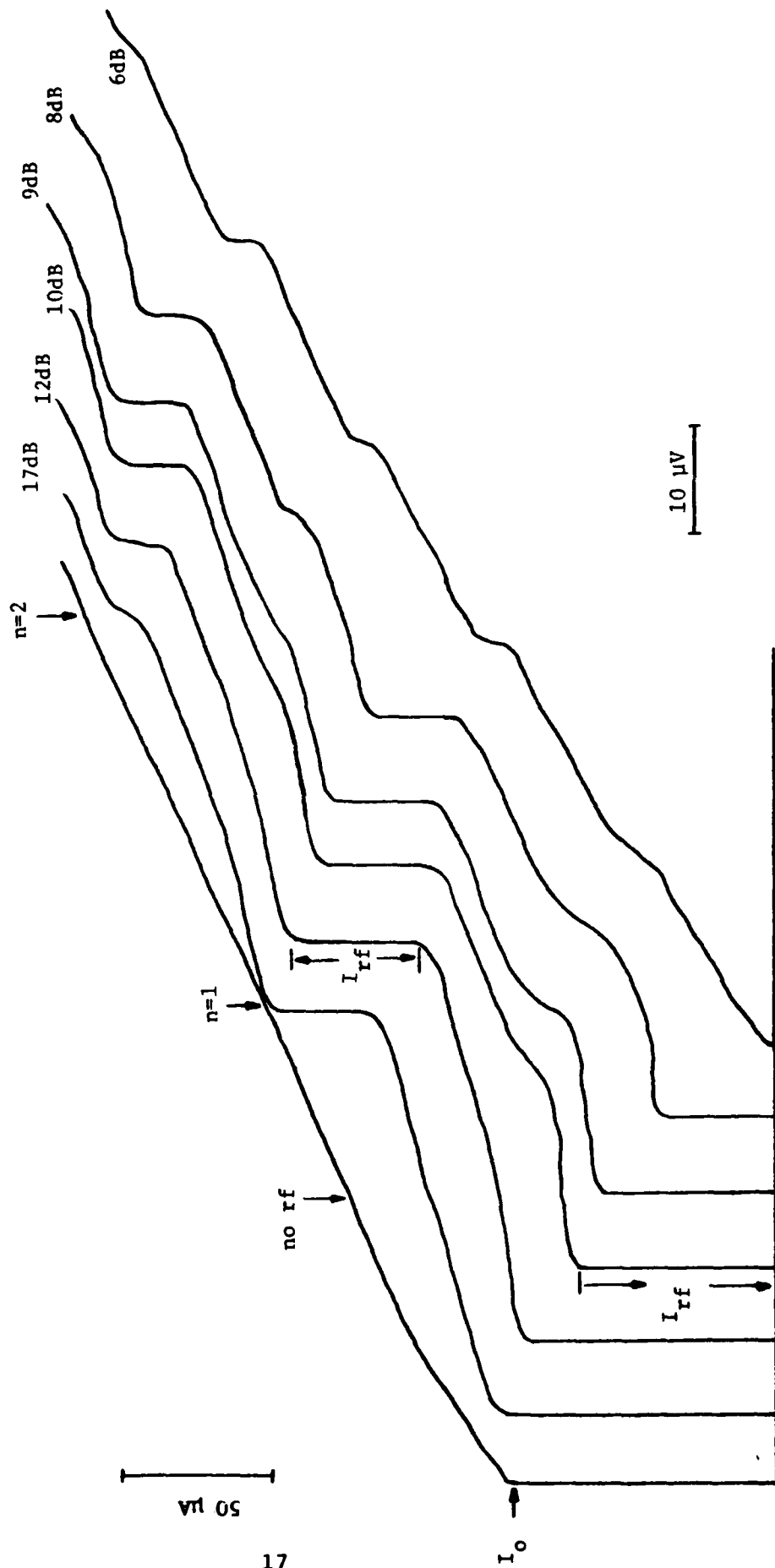
no rf

I_{rf}

50 μA

I_o

Figure 5. Typical Microbridge Characteristics Curves, with and without Microwave Perturbation
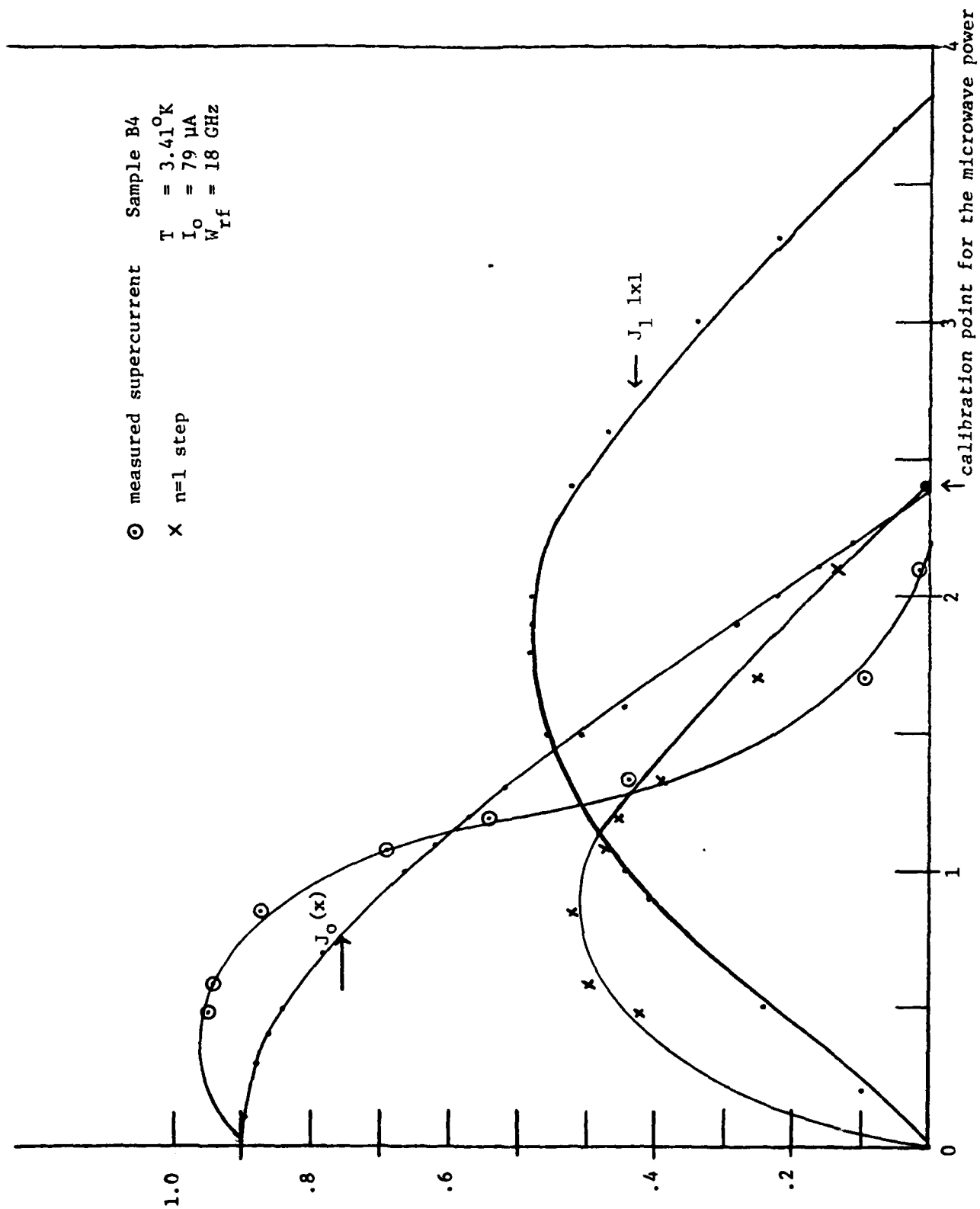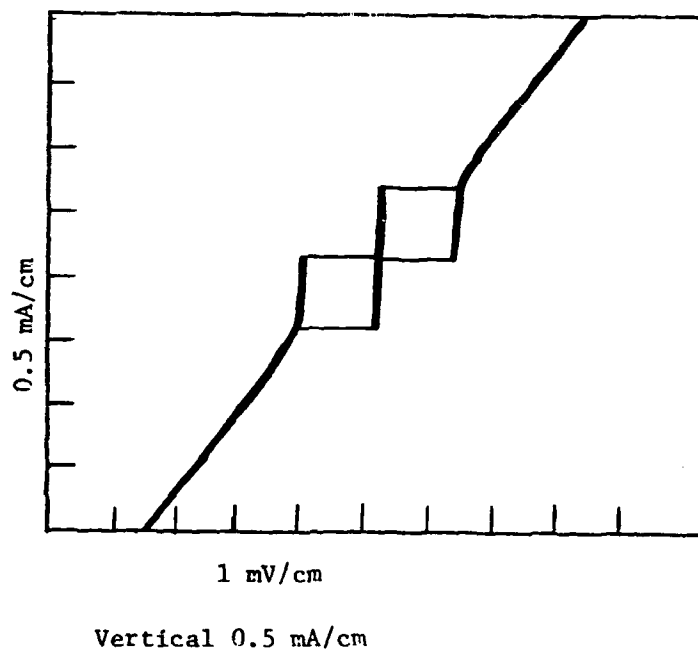
Figure 6. Power Dependence of the Josephson Supercurrent

18

Figure 7.   Characteristics Curves
            Josephson Junctions (T = 1.34°K)

19

also shows nice quasiparticle tunneling characteristics with a
negligible leakage current.

There are some differences between the characteristics of micro-
bridge and tunnel junctions that should be recognized. Microbridges
do not show hysteresis as do tunnel junctions. This is because
tunnel junctions have a much higher capacitance.[9,10] Whether a
hysteresis is desirable or not depends on the application. In
the case of digital applications, hysterisis is usually desirable.
While for detector applications, non-hysteresis junction perform-
ance is usually desirable. Smaller tunnel junctions, with neglig-
ible capacitance, also show negligible hysteresis.

III.1.3 Quasiparticle Injection Non-equilibrium States: This study
resulted in some very interesting observations of multilayer tunnel
junction behavior. The device structure is lead (1200.Å)-tin(200 Å)-
tin oxide-tin(200 Å)-lead(1200 Å). Since the tin film is only 200 Å,
it is not perfectly uniform.

It can be assumed that there are some lead islands on the tin
oxide, therefore, we can see quasiparticle tunneling between lead
and tin. Due to the proximity effect, the transition temperature
of the tin with the lead islands will be somewhat higher than pure
tin. At a finite voltage, quasiparticles injected from one side of
the junction to the intermediate layer of the other side will change
the excitation spectrum; this will give some extra structures in the
quasiparticle tunneling curve. As shown by the data of Figure 8,
such complicated structures have indeed been observed.

These observed current-voltage characteristics are believed to
be the first of its kind. Additional experiments confirmed that
the results are reproducible. At this time, there is no available
theory to compare with the results but it is believed that the
interpretation given above is a plausible one.
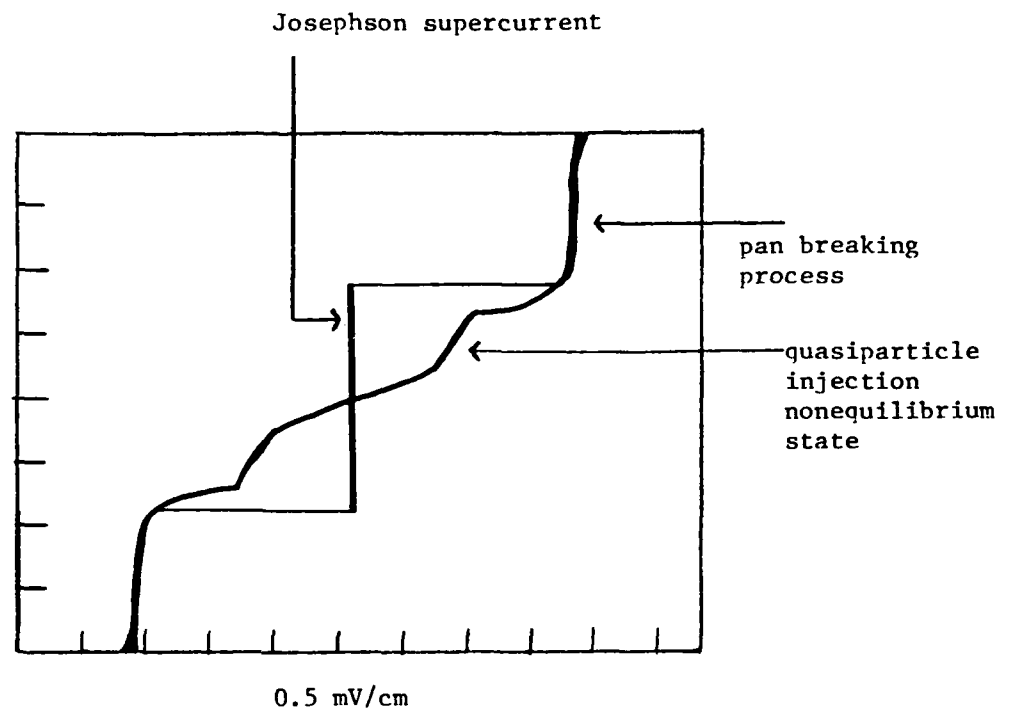
Josephson supercurrent

pan breaking process

quasiparticle injection nonequilibrium state

0.5 mV/cm

Figure 8. Characteristics Curve of Multi-layer Tunnel Junction Showing the Effect of Quasiparticle Injection (T = 3.60°K)

21

Further investigations of this nature may prove to be very productive. The highly nonlinear region that results from the quasiparticle injection non-equilibrium states is not accessible in a one-layer tunnel junction.

III.2 Structure and Grain-Size Modification of Nb Thin Films by Laser Annealing

Experiments were conducted to determine how to control the grain size of superconducting thin films, since grain boundary effects and impurities localized in grain boundaries can affect the superconducting films. Of particular interest, were experiments to assess whether laser-annealing-assisted growth of grains could be used to substantially alter the structure of the thin films. These experiments were suggested by the observation here and in other laboratories of significant increases in grain size after laser annealing of non-superconducting thin films.[11-13]

III.2.1 Sample Preparation: Test samples used in these experiments consisted of niobium (Nb) thin films (1000 $\overset{o}{A}$) deposited on single-crystal Si wafers of (100) orientations on thin-film Si_3N_4 layers on Si substrates. Both sputtering and e-beam evaporation were used in depositing the Nb films.

Laser-annealing experiments were conducted using the ARACOR CW laser annealing system. This system uses a 20 W Argon laser. The sample is positioned on a vacuum chuck, which can be accurately heated over the temperature range of 0 to 400°C. The motion of the sample stage can be programmed and moves on an air bearing at rates of up to 25 cm/sec in both the x and y directions.

In the experiment of this program, the laser power was varied from 0.5W to 8W in 0.5W increments. The sample scanning rate and the laser beam spot size were fixed at 10 cm/sec and 40 μm, respectively. The substrate temperature was held at 250°C.

After laser annealing, the samples were cut into 3mm x 3mm squares and prepared for examination in a transmission electron microscope (TEM). Samples were prepared for TEM analysis by chemical jet thinning through the Si substrate. The interfacial Si_3N_4 layers were removed either by chemical etching or ion milling. The TEM examinations were performed on the ARACOR Simens 102 Electron Microscope operated at 125 keV.

III.2.2 <u>Experimental Results</u>: Initial results obtained on Nb thin films on single-crystal Si substrates indicated that regions of substantial grain growth had occurred after laser annealing. However, pronounced evidence of pitting was observed, implying indiffusion of Nb. Correlated Auger electron spectroscopy profiling confirmed that significant interdiffusions of Nb and Si had occurred, resulting in the observed surface degradation after laser irradiation.

To overcome the problem of surface reactions between the Nb and Si, a 500 Å thick Si_3N_4 layer was deposited on the Si surface before depositing the Nb film. TEM examination of the sputtered (as-deposited) Nb films on Si_3N_4 indicated the presence of a fine-grained polycrystalline structure. The transmission electron micrograph in Figure 9 shows that the average grain size is less than 100 Å. The diffraction pattern (Figure 10) confirms that a fine-grained structure is present with an apparent absence of long-range ordering.

Corresponding examination of electron-beam-evaporated films showed that grains of $\sim$ 1000 Å average size are present, as shown in the bright-field electron micrograph of Figure 11. The selected-area diffraction pattern shown in Figure 12 also indicates the presence of distinct crystallites and an absence of fine-grained structure.

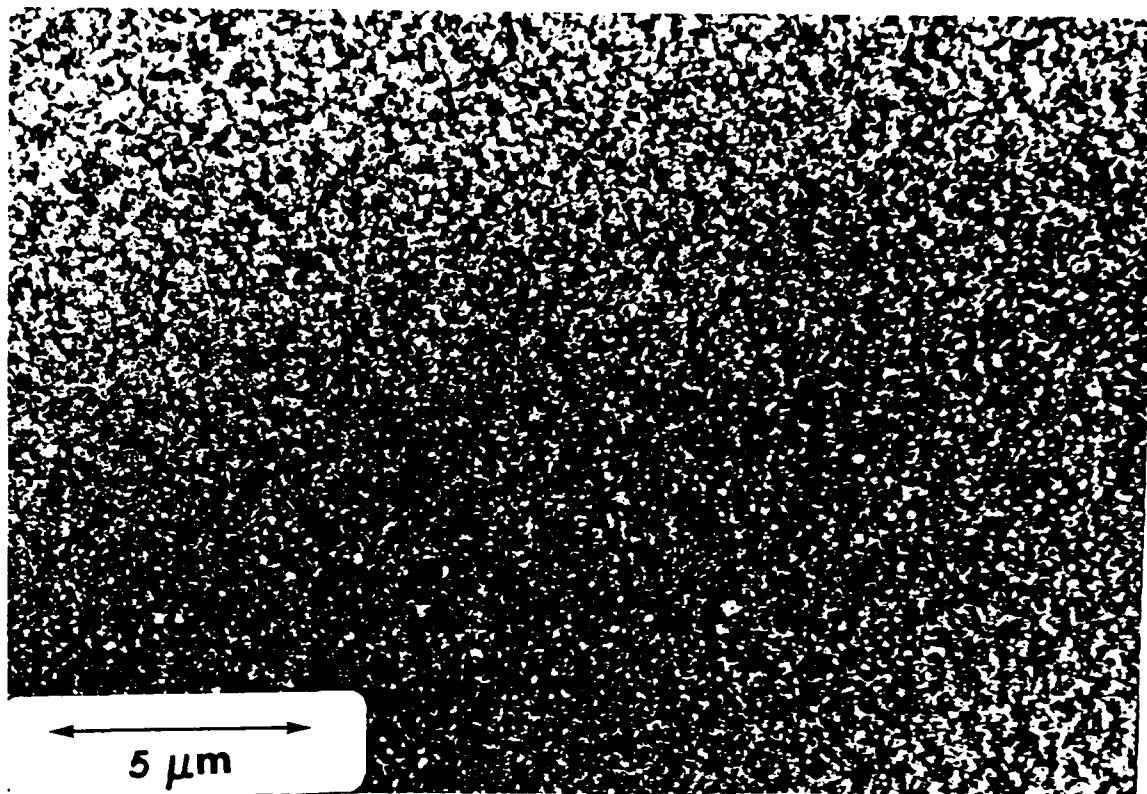**5 μm**

Figure 9.   Transmission Electron Micrograph of
            Film Sputter-Deposited

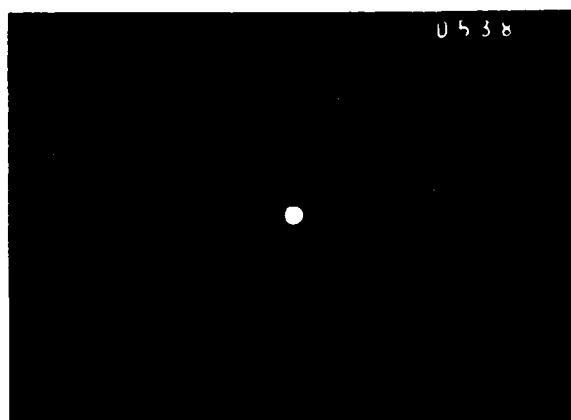

U 5 3 8

Figure 10.   Electron Diffraction Pattern of the
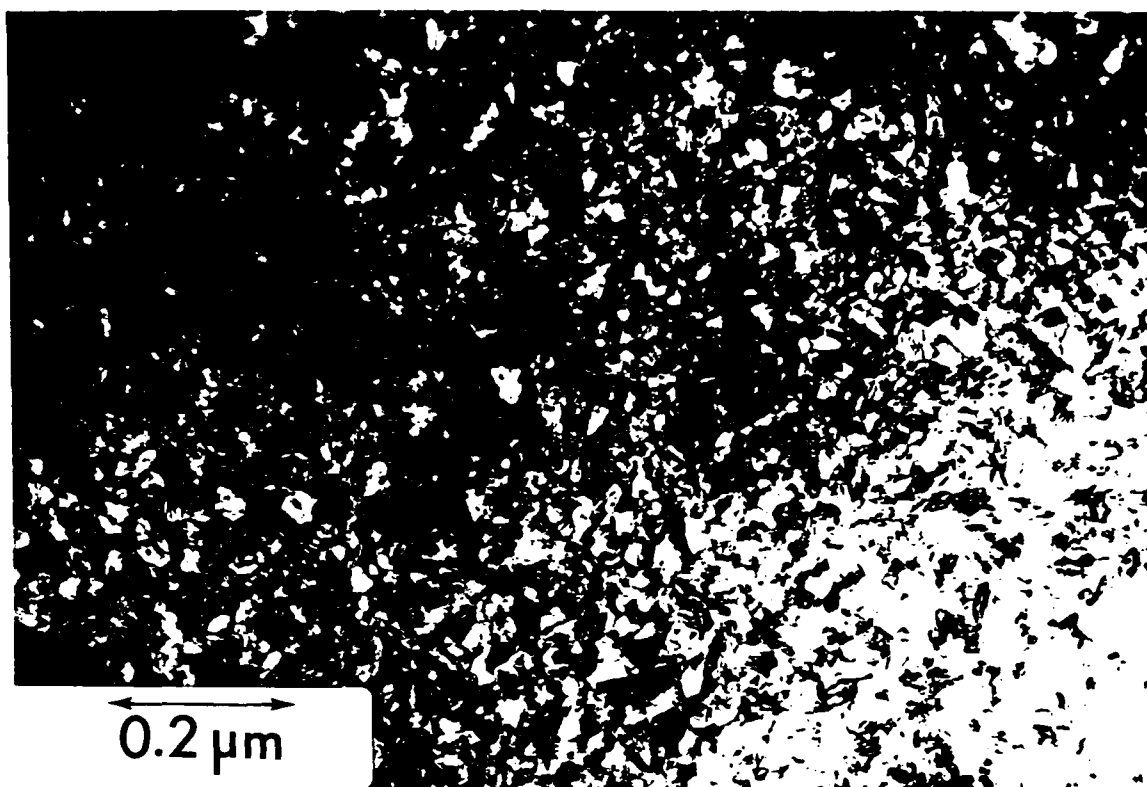   Film shown in Figure 9

Figure 11. Transmission Electron Micrograph
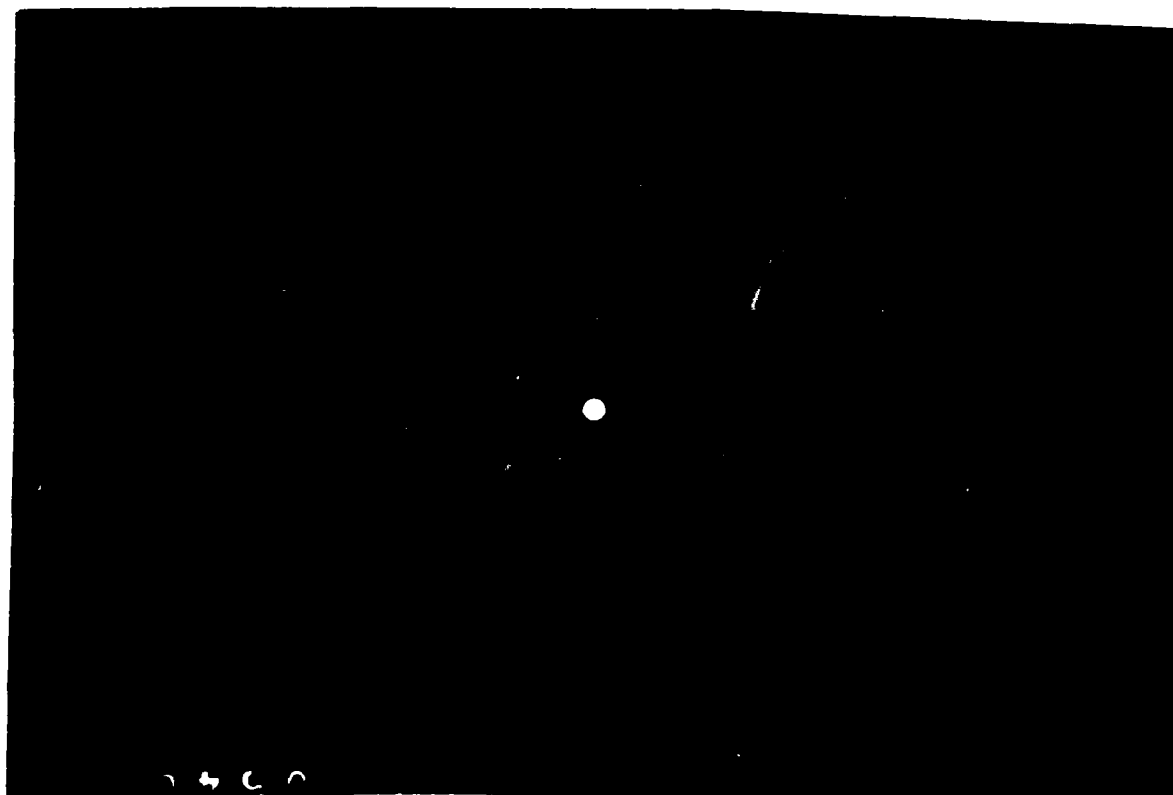of Electron-Beam-Evaporated Film

Figure 12. Electron Diffraction Pattern of the
Film shown in Figure 11

After exposure of the Nb films to laser powers in the range 0.5W to 3W, it was found that no significant alteration in polycrystalline structure had occurred. At 4W, a number of large crystallites are observed within the fine-grained matrix after laser annealing. A representative bright-field electron micrograph, obtained within a laser-scanned region, is shown in Figure 12. It is observed that large grains with a maximum size of $\sim$ 2 μm are developed in these zones. However, large areas contain fine-grained material and the large grains are not uniformly distributed.

After exposing the samples to a laser power of 5W, a uniformly-developed film of large crystallites is detected. In Figure 14, the dark-field electron micrograph shows well-defined crystallites of average dimensions, 5 μm x 10 μm, with no evidence of fine-grained polycrystalline structure remaining in the film. Corresponding selected-area electron diffraction patterns confirm the presence of large crystallites of varying orientation.

Increasing the laser power to 6W results in the formation of voids at the surface of the film, as shown in Figure 15. These voids are attributed to localized vaporization of the material on non-uniform absorption regions. At laser powers exceeding 6W, delamination and peeling of the film structure occurs.

From the data obtained, we can conclude that scanning laser annealing at laser power levels $\leq$ 3W produces no significant increase in grain size, since insufficient thermal energy is present to initiate grain growth. At 4W, the presences of large grains interspersed within the fine-grained matrix indicates that melting has occurred within localized regions and regrowth has been initiated at the $Nb-Si_3N_4$ interface. An additional increase in the laser power to 5W produces complete melting and recrystallization of the film, resulting in column structures extending from the nitride interface to the surface of the film. For laser powers $\geq$ 6W, severe surface degradation is caused by vaporization and thermal crazing.
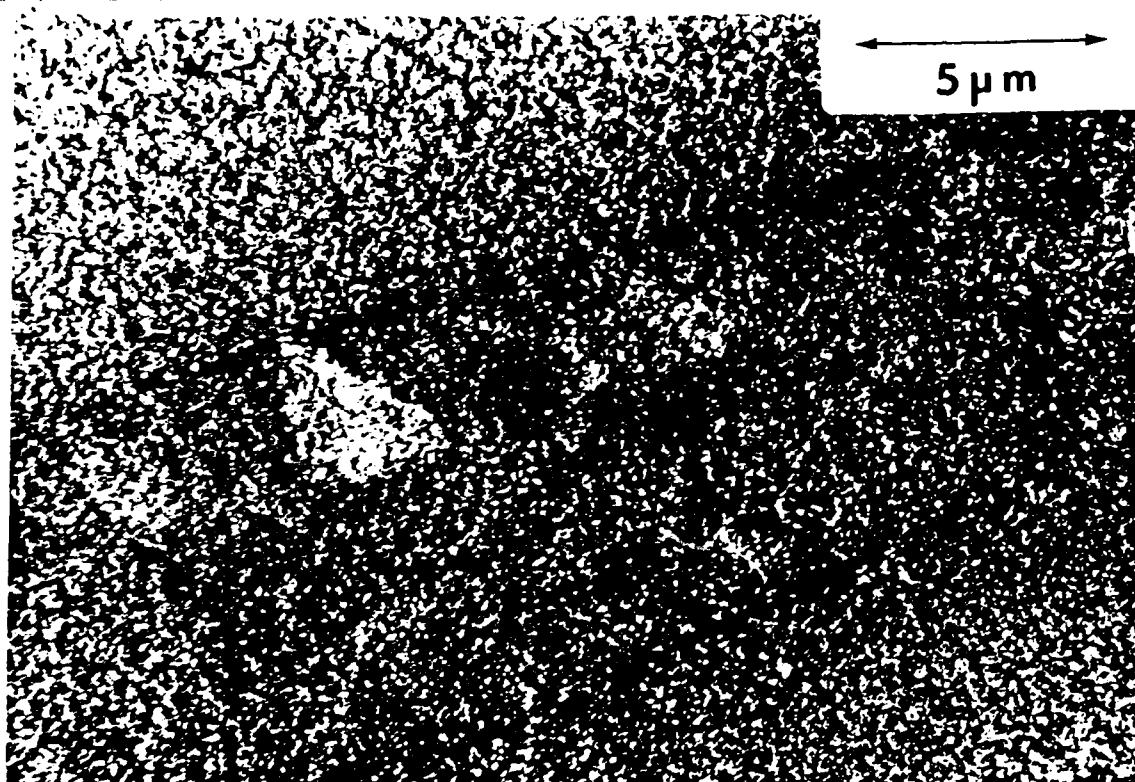
26

Figure 13. Bright-Field Electron Micrograph of
Film Laser Annealed at Low Power
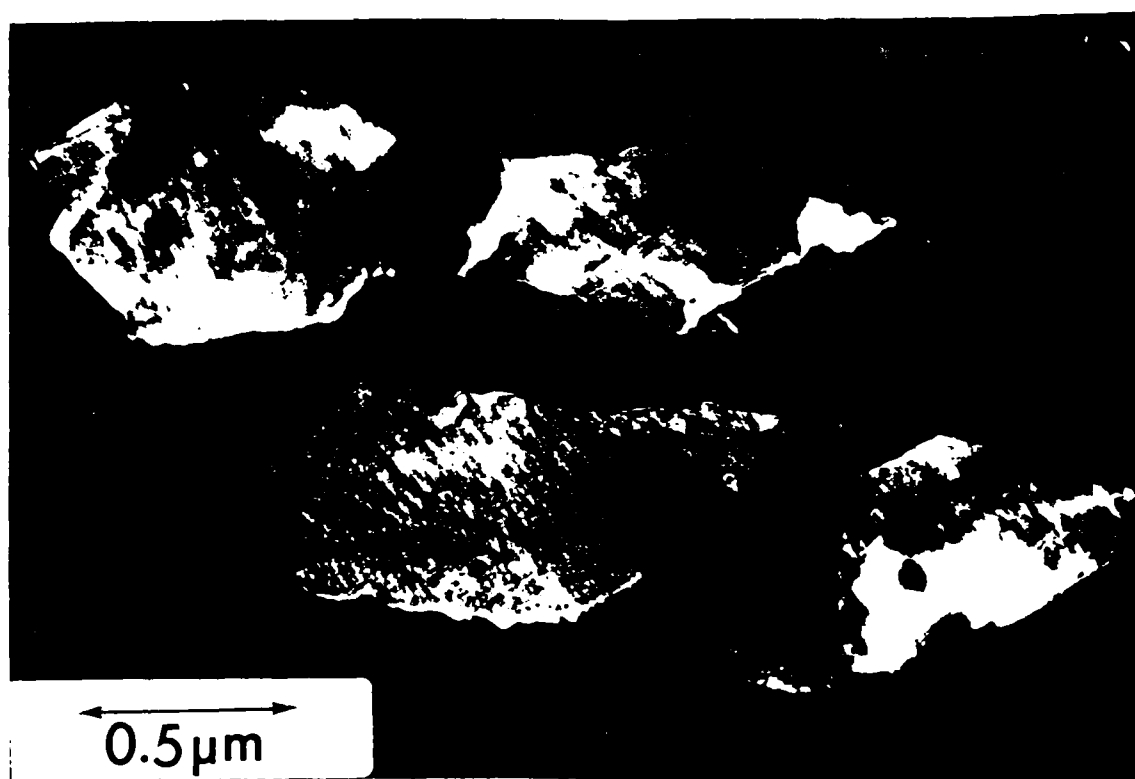(0.5 to 3w)

Figure 14. Dark-Field Electron Micrograph of
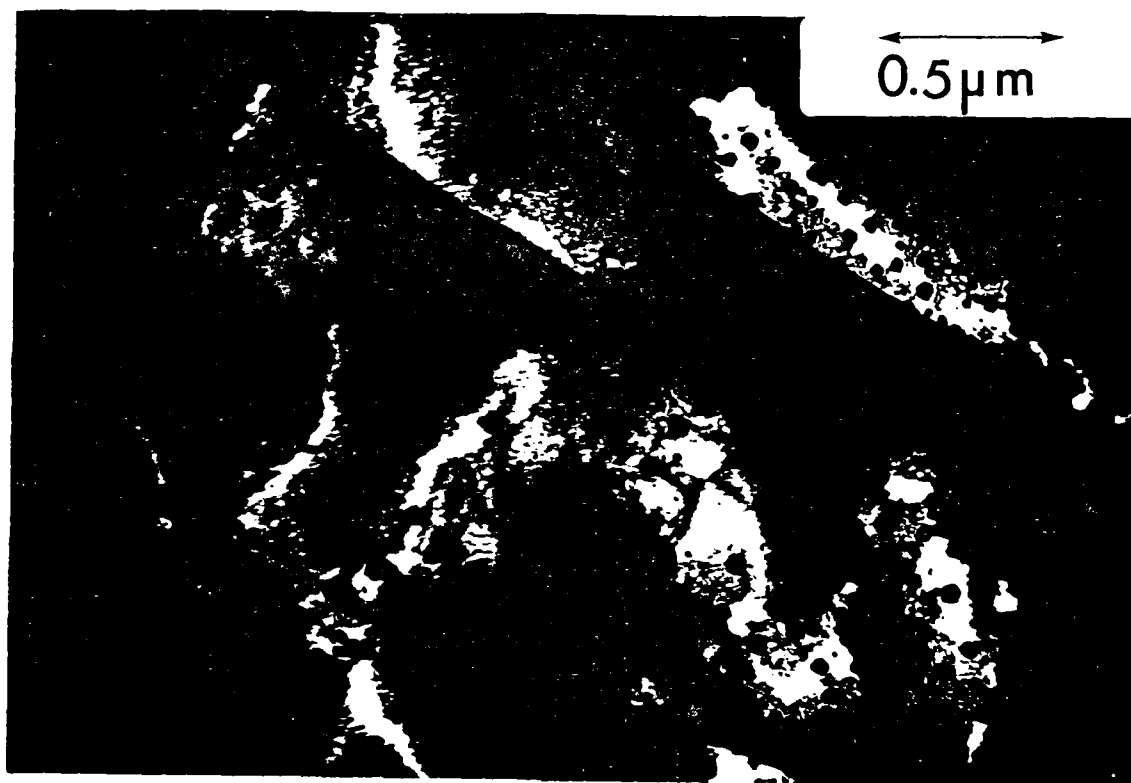Film Laser Annealed at Intermediate
Powers (5w)

27

Figure 15.   Dark-Field Electron Micrograph of
Film Laser Annealed at Higher Powers (6w)

IV. DISCUSSION OF RESULTS AND CONCLUSIONS

In this research program, non-equilibrium states were observed in microwave-irradiated thin-film microbridges. Quasiparticle injection phenomena in Josephson tunnel junctions was also studied. The enhancement of supercurrents due to microwave irradiation is of great fundamental interest for it clearly shows that the pairing process is sensitive to external perturbations. Quasiparticle injection in tunnel junctions indicates a redistribution of the quasiparticle spectrum, which may lead to an increase in the superconducting transition temperature. It is hoped that more extensive studies of these phenomena will lead to a better understanding of the superconducting states.

In general, we have seen that those non-equilibrium states created by microwave irradiation and quasiparticle injection will change the current-voltage characteristics of Josephson devices. This certainly will affect the sensitivity of such devices. The fabrication of an ideal Josephson device, suitable for high-frequency applications, remains a challenging topic.

The experiments on the control and increase of the grain size of Nb superconducting films showed that the grain size is somewhat dependent on the deposition technique that is chosen. However, the various deposition choices only resulted in changes in grain size on the order of 1000 $\overset{\circ}{A}$.

Laser annealing of the deposited films, however, resulted in substantial modifications to the structure of the Nb films. With proper laser annealing techniques, relatively fine-grained poly-crystalline films can be virtually entirely converted to large polycrystalline grains with an average size of approximately 5 μm x 10 μm. For both theoretical and practical reasons, it would be interesting to evaluate the effect of controlled changes in the film structure on superconducting properties over the wide range afforded by post-deposition laser annealing of the film; such a study was, however, beyond the scope of this program.

29

V. REFERENCES

1. J. Bardeen, L. N. Cooper, and J. R. Schrieffer, Phys. Rev. 108, 1175 (1957).

2. B. D. Josephson, Adv. Phys. 14, 419 (1965).

3. J. C. Solinsky and T. C. Wang, "A Study of Low Temperature processes in Non-equlibrium Electronic States." ARACOR proposal # PDGP-78-37, October 9, 1978.

4. G. M. Eliasberg, JETP Letters, 11, 114 (1970).

5. G. M. Eliasberg, Sov. Phys. JETP 34, 668 (1972).

6. B. I. Ivlev and G. M. Eliasberg, JETP Letters 13, 333 (1971).

7. B. I. Ivelv and S. G. Lisitsyn and G. M. Eliasberg, J. Low Temp. Phys. 10, 449 (1973).

8. Beth Stoeckly, "Transient in Nonequilibrium Superconductors," Phys. Rev. B preprint.

9. W. C. Stewart, Appl. Phys. Lett. 12, 277 (1968).

10. D. E. McCumber, J. Appl. Phys. 39, 3113 (1968).

11. A. Gat, et al, Appl. Phys. Lett, 34, 831 (1979).

12. J. F. Gibbons, et al., Appl. Phys. Lett, 34, 831 (1979).

13. J. Peng, unpublished data.

APPENDIX   A

CURRENT-DENSITY DISTRIBUTION IN JOSEPHSON TUNNEL JUNCTIONS

Current-density distribution in Josephson tunnel junctions

T. C. Wang

Advanced Research and Applications Corporation, Sunnyvale, California 94086

An analysis of the relation between current-density distribution and the peak amplitude of Fiske modes in Josephson junctions is presented. It is shown that the peak value can vary through a large range of values, depending on whether the junction is "good" or "bad" in the sense of the uniformity of the oxidation barrier. By a close examination of the Fiske modes, it is possible to determine the barrier uniformity. However, for a nonuniform barrier junction, the current-density distribution corresponding to a particular field dependence of Fiske modes is no longer unique. A method of evaluating junctions for use as electronic devices is discussed.

I. INTRODUCTION

Current-density distribution in a Josephson tunnel junction is one of the most important factors in determining device performance; however, an unambiguous method of determining this distribution has yet to be found. Since the spatial variation of the order parameter phase difference ϕ across the junction barrier is a function of magnetic field, the most straightforward and powerful method to determine the current-density distribution $J(z)$ is to study the magnetic field dependence of Josephson currents. This approach has been suggested by Dynes and Fulton[1] to extract the information of the current-density profile from the field dependence of Josephson critical currents. It was shown by Zappe[2] that such a determination is not unique unless an additional hypothesis is made. Important work in Josephson junctions was done by Matisoo[3] who studied current-density distributions in large junctions (where the junction length L was much greater than the penetration depth λ_j) and demonstrated that nonuniform current-density distribution existed in the presence of a vortex flux structure. Basavaiah *et al.*[4] used both ellipsometric and tunneling methods to measure the junction barrier thickness. They showed that the current density is an extremely sensitive function of the barrier thickness. A variation of about 4 Å can change the current density by one order of magnitude. More recently, Barone *et al.*[5] considered the case of nonuniform current-density distribution and its effect on the diffraction pattern in Josephson junctions. Russo and Vaglio[6] extended the case to include effects on Fiske modes.

Fiske modes are due to a nonlinear interaction between the Josephson current-density waves and electromagnetic standing waves in the junction cavity. The amplitude of Fiske modes are given by[7]

$$J_{dc} = \lim_{T \to \infty} \frac{1}{T} \int_0^T dt \frac{1}{L} \int_0^L dz\, J(z) \sin\phi\,(z,t), \qquad (1)$$

where ϕ is a function of the spatial coordinate z and the time t, and L is the junction's length along the z direction.

In principle, one should be able to extract the current-density profile $J(z)$ from the magnetic field dependence of J_{dc}

by an inversion of Eq. (1). Sections II–IV discuss such a method.

II. THEORY

In the case of an arbitrary current-density distribution, the behavior of Fiske modes is described by the following differential equation.[6]

$$\frac{\partial^2 \phi}{\partial z^2} - \frac{1}{\bar{c}^2}\left(\frac{\partial^2 \phi}{\partial t^2} + \gamma \frac{\partial \phi}{\partial t}\right) = \frac{J(z)}{\langle J \rangle} \frac{1}{\lambda_j^2} \sin\phi \qquad (2)$$

The magnetic field is applied along the y direction. The Josephson current density $J(z)$ is along the x direction and ϕ, the phase difference, is a function of z and t. $\bar{c}$ is the phase velocity of the electromagnetic wave in the junction. $\lambda_j^2 = \hbar c^2 / 16\pi e \lambda_L \langle J \rangle$ is the Josephson penetration depth; λ_L is the London penetration depth. γ is the damping constant and is related to the junction's quality factor Q by the relation $Q = \omega / \gamma$. ω is the frequency of the Fiske mode. $\langle J \rangle$ is the average value of $J(z)$ over the junction area A ($= WL$) and W is the junction width along the y direction.

Kulik[7] used perturbation methods to solve Eq. (2) and rigid boundary conditions. His boundary conditions were for total reflection of electromagnetic waves at the junction edges, and his results were that the current in the junction I_n is determined by

$$I_n = I_0 J_0(\tfrac{1}{2}a) J_1(\tfrac{1}{2}a) F_n(r), \qquad (3)$$

where

$$F_n(r) = \frac{1}{\langle J \rangle} \left| \frac{2}{L} \int_0^L J(z) \exp\left(i\frac{2\pi r}{L} z\right) \cos\left(\frac{n\pi r}{L}\right) dz \right|. \qquad (4)$$

The parameter a is determined by

$$J_0^2(\tfrac{1}{2}a) = a/z_n F_n, \qquad (5)$$

where J_n are Bessel functions. I_n is the magnitude of the nth Fiske mode, and n, an integer, is the mode number. $I_0 = \langle J \rangle A$ is the junction critical current at zero field. r is equal to H_{appl}/H_0. H_{appl} is the applied magnetic field and H_0 is the field value producing one flux quantum in the junction. The parameter z_n introduced by Kulik is related to the qual-
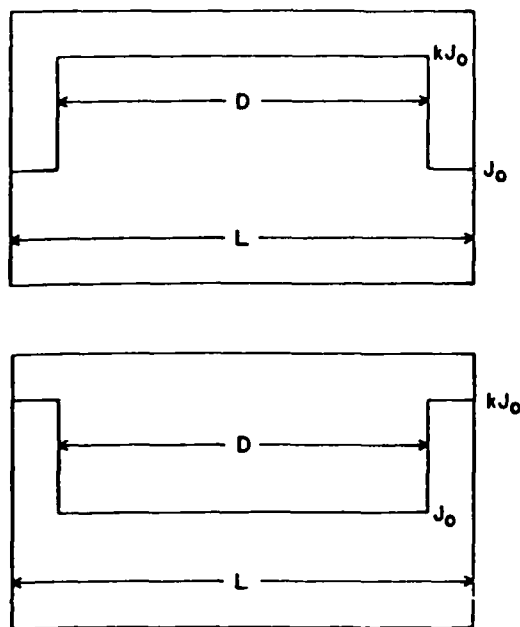
FIG. 1. Two possible types of current-density distributions in a real Josephson junction. L is the length of the junction, while k and D are treated as variables. (a) has a higher current density in the middle, while (b) has a higher current density at the edges of the junction.

ity factor of the nth mode Q_n by $z_n = Q_n(L/n\pi\lambda_J)^2$. F_n determines the field dependence of Fiske modes.
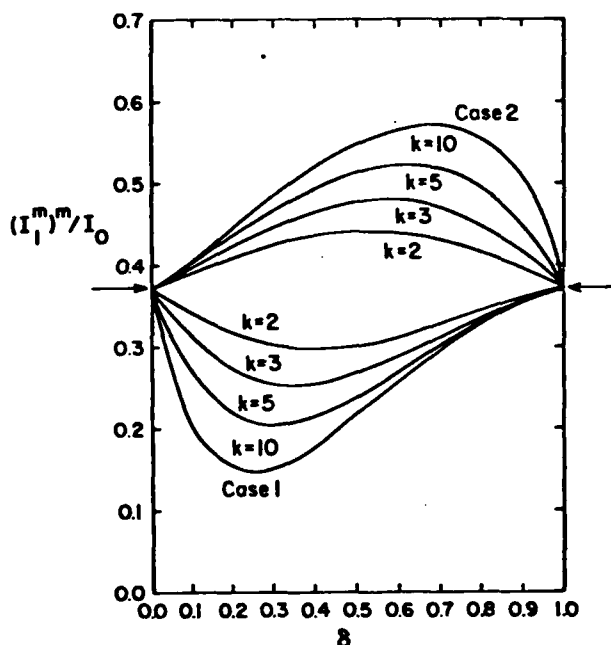
It is worth noting that Eq. (4), which determines the

FIG. 2. The maximum values of I_1^m versus δ for different values of k for $n = 1$ mode. I_1^m is the maximum amplitude of Fiske steps as a function of magnetic field at a specific temperature. $(I_1^m)^m$ is the maximum value of I_1^m as a function of temperature. The curves are calculated based on Eq. (6), and using the relation $(I_n^m)^m/I_0 F_n^{max} = 0.34$. Case 1 and case 2 correspond to the current-density distribution in Figs. 1(a) and 1(b), respectively. The arrows in this figure and in Figs. 3 and 4 mark Kulik's results of uniform junctions.
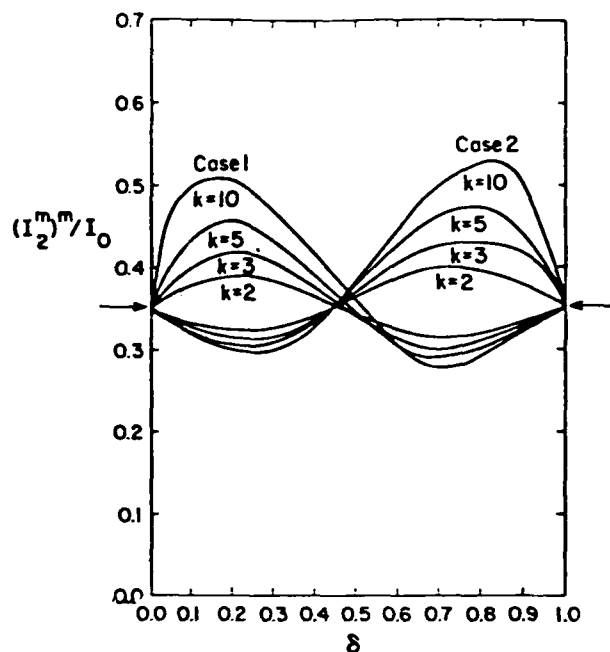

FIG. 3. The maximum values of I_n^m versus δ for different values of k for $n = 2$ mode.

amplitude and field dependence of Fiske modes, is just the Fourier transform of $J(z)$ multiplied by $\cos(n\pi z/L)$. $J(z)$ is the amplitude of the Josephson current-density waves in the presence of constant voltage and magnetic field in the junction, and $\cos(n\pi z/L)$ is proportional to the amplitude of the electromagnetic standing waves in the junction cavity. This is the nonlinear Fiske mode interaction between the waves.

The general feature of Fiske modes is that, at a certain temperature, the field-dependent Fiske modes have a maximum I_n^m for a particular value of magnetic field. As the temperature decreases, the junction's Q_n increases and the maximum amplitude I_n^m first increases, reaches a maximum $(I_n^m)^m$, and then decreases again as Q_n increases further.[8-10]

In the theory, $(I_n^m)^m$ is determined by the universal relation of $I_n/I_0 F_n$ versus $z_n F_n$. (See Fig. 2 in Ref. 8) This can be seen easily by eliminating the parameter a in Eqs. (3) and (5). For all cases, $(I_n^m)^m/I_0 F_n^{max} = 0.34$.

III. TWO LIMITING CASES OF CURRENT-DENSITY DISTRIBUTION

In Sec. II, a general solution for Fiske modes was presented. In the following discussion, we consider two arbitrary types of current-density distributions as shown in Figs. 1(a) and 1(b), referred to as case 1 and case 2, respectively.

For these two types of current-density distribution, Eq. (4) gives case 1 as

$$F_n(r) = \frac{1}{1 + (k-1)\delta} \left| \frac{2r}{\pi} \frac{\sin(r - \frac{1}{2}n)\pi}{r^2 - (\frac{1}{2}n)^2} + (k-1) \right.$$

$$\left. \times \frac{\sin(r - \frac{1}{2}n)\pi\delta}{\pi(r - \frac{1}{2}n)} + \frac{(-1)^n \sin(r + \frac{1}{2}n)\pi\delta}{\pi(r + \frac{1}{2}n)} \right| \quad (6a)$$

FIG. 4. The maximum values of I_n^m versus δ for different values of k for $n = 3$ mode.

and case 2 as

$$F_n(r) = \left(1 - \frac{(k-1)}{k}\delta\right)^{-1}\left|\frac{2r}{\pi}\frac{\sin(r - \frac{1}{2}n)\pi}{r^2 - (\frac{1}{2}n)^2} - \frac{(k-1)}{k}\right.$$

$$\left.\times\frac{\sin(r - \frac{1}{2}n)\pi\delta}{\pi(r - \frac{1}{2}n)} + \frac{(-1)^n\sin(r + \frac{1}{2}n)\pi\delta}{\pi(r + \frac{1}{2}n)}\right|. \quad (6b)$$
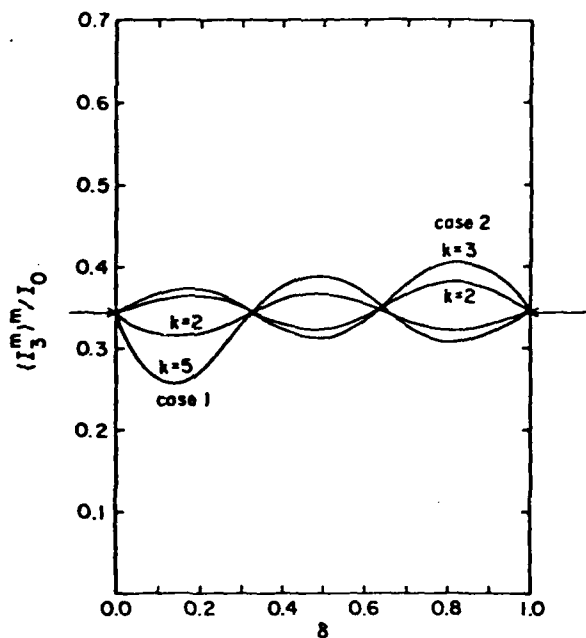
Here, δ ($= D/L$) and k are parameters describing the nonuniformity of the junction oxidation barrier $(0 < \delta < 1, k > 1)$. D and k are defined in Figs. 1(a) and 1(b).

Figures 2,3, and 4 show the results for $(I_n^m)^m/I_0$ for $n = 1, n = 2$, and $n = 3$ modes for various values of k and δ, based on Eq. (6). In the limit of both $\delta = 0$ and $\delta = 1$, which corresponds to the case of uniform current distribution, the results reduce to Kulik's value, marked by the arrow in the Figs. 2–4.

There are several interesting features that should be noted. First, the maximum values of I_n^m/I_0 can vary over a large range of values, namely, from 0.06 to 0.68 in the limit of k going to infinity. Second, the magnetic field which maximizes the modes for most cases does not differ much (less than 10%) from Kulik's results. However, for $k = 10$ and δ between 0.4 and 0.6 in case 1, it is found that the field which maximizes the $n = 2$ mode is even smaller than the field which maximizes the $n = 1$ mode. This result differs from Kulik's results for uniform current-density distribution. The quantity most sensitive to changes in the current-density distribution is $(I_n^m)^m/I_0$, and thus, we will use this quantity to extract information on $J(z)$.

IV. APPLICATIONS OF THE THEORETICAL RESULTS TO REAL JUNCTIONS

The sensitivity of the ratio $(I_n^m)^m/I_0$ on current-density determined will be compared with previous experimental measurements on Fiske modes by the author. All the examples discussed in the following paragraphs are concerned with small junctions, i.e., $L < 2\lambda_J$. Using sample N26 in Ref. 9 as an example of a "good" or uniform case, the measured values are $(I_1^m)^m/I_0 = 0.38$, $(I_2^m)^m/I_0 = 0.34$ and $(I_3^m)^m/I_0 = 0.35$. of Fig. 2 shows that more than one choice of the current-density distribution can be made to yield the same ratio. However, for a particular choice of k and δ, it does not necessarily result in correct amplitudes for the $n = 2$ and $n = 3$ modes from Figs. 3 and 4. A closer examination shows that $k = 2$ and $\delta = 0.06$ in case 2 are more plausible. This choice results in $(I_1^m)^m/I_0 = 0.38$, $(I_2^m)^m/I_0 = 0.34$, and $(I_3^m)^m/I_0 = 0.35$. However, there are also other choices possible that have agreeable ratios. For example, $k = 3$ and $\delta = 0.04$ in case 2 will give $(I_1^m)^m/I_0 = 0.38$, $(I_2^m)^m/I_0 = 0.34$, and $(I_3^m)^m/I_0 = 0.355$, which differs little from the previous k and δ results. For higher values of k, i.e., $k = 10$ and any value of δ, it is not possible to find a corresponding current-density distribution which will give all three modes the correct amplitude. Therefore, even though the choice is not unique, we are able to conclude that the actual current-density distribution of the sample should be close to a small k value in case 2. Combining this result with the current-density profile extracted from the diffraction pattern (which indicated that this sample had a uniform current density over 90% of the junction area, and then increased a small amount, then decreased to zero gradually at the edges of the junction) indicates that this sample's oxidation barrier is indeed uniform.

In the "bad" case, such as sample N28 in Ref. 9, the values are $(I_1^m)^m/I_0 = 0.36$, $(I_2^m)^m/I_0 = 0.36$, and the small value of $(I_3^m)^m/I_0 = 0.18$. These values, combined with the junction's unusual field dependence of the $n = 1$ mode, suggest that the junction had an irregular current-density distribution. In this case, no detailed information about the actual current-density profile can be extracted.

For all the other samples in Refs. 8 and 9, Q_n is not high enough to observe the peak values of higher-order modes, and hence, no detailed information on the current-density distribution can be deduced from Fiske modes. However, because the peak values of the $n = 1$ mode were always between 0.35 and 0.38, the junction exhibited a uniform diffraction pattern of Josephson critical current and an appropriate field dependence of Fiske modes: the data suggest that the oxidation barriers were uniform.

V. SUMMARY

In summary, we have demonstrated that by studying the field dependence of Fiske modes, it should be possible to tell how uniform the oxidation barrier of a Josephson tunnel junction is, but that there is no unique current-density distri-

bution that corresponds to a particular observed field dependence.

It will be interesting to fabricate junctions of the type of oxidation barrier discussed in the text and compare results with the calculations. The desired junctions can be fabricated by rf sputter etching[11] of a uniform junction through a patterned mask to thin a certain portion of the oxidation barrier before the deposition of the counterelectrode. This kind of information might be useful for making practical microwave devices.

For example, Fig. 2 shows that junctions with lower current density at the edges always give weaker fundamental-mode performance than a uniform junction, while junctions with higher current densities at the edges give stronger fundamental-mode performances. The second type of junction would be more useful for microwave devices operating in the fundamental mode. As another example, Figs. 2 and 3 together show that for a junction with lower current density at the edges with large k and small δ, the second-harmonic mode will be stronger than the fundamental. This type of junction will be useful for devices using the second-harmonic mode. Such a method of evaluating junctions for possible use as microwave devices should be studied further.

[1]R.C. Dynes and T.A. Fulton, Phys. Rev. B 3, 3015 (1971).
[2]H.H. Zappe, Phys. Rev. B 11, 2535 (1975).
[3]J. Matisoo, Appl. Phys. 40, 1813 (1969).
[4]S. Basavaiah, J.M. Eldridge, and J. Matisoo, J. Appl. Phys. 45, 457 (1974).
[5]A. Barone, G. Paterno, M. Russo, and R. Vaglio, Phys. Status Solid 41A, 393 (1977).
[6]M. Russo and R. Vaglio, Phys. Rev. B 17, 2171 (1978).
[7]I.O. Kulik, Zh. Eksp. Teor. Fiz. Pis ma Red. 2, 134 (1965); Sov. Phys.-JETP Lett. 2, 84 (1965); Zh. Tek. Fiz. 37, 157 (1967); Sov. Phys.-Tech. Phys. 12, 111 (1967).
[8]Y.S. Gou and R.I. Gayley, Phys. Rev. B. 10, 4584 (1974).
[9]T.C. Wang and R.I. Gayley, Phys. Rev. B. 18, 293 (1978).
[10]R.F. Broom and P. Wolf, Phys. Rev. B 16, 3100 (1977).
[11]J.H. Greiner, J. Appl. Phys. 42, 5151 (1971).

APPENDIX   B

GETTING TO THE COMPETITIVE MARKETPLACE WITH
JOSEPHSON JUNCTION DEVICES

GETTING TO THE COMPETITIVE MARKETPLACE WITH JOSEPHSON JUNCTION DEVICES[*]

By: J. C. Solinsky

March 22, 1978

ABSTRACT

An opinion is presented to stimulate low temperature device development
in the computer device area. The marketplace for Josephson junction devices,
with present research progress, points to a slight technically competitive
edge over semiconductor devices in the 1990 computer device time frame.
However, it is projected that such a marketplace will only materialize
if the cost of Josephson devices is quite competitive. Unless industrial
and present federal funding in Josephson and other low temperature device
research is dramatically increased and the research is pursued in a competitive
manner, the Josephson computer may not be competitive with semiconductor
devices. It also may be only available from a single manufacturer and supplied
to specialized government clients. An alternative to this projection is to
stimulate industrial funding through the education of future computer device
design engineers. These engineers can argue the merits for low temperature
devices in a competitive manner to industrial management.

Introduction

Most people who have worked in the field of superconductivity are
quite captivated with the theoretical description and experimentally
verified processes that occur in Josephson and other low temperature
devices. Not only have many types of quasi-particle processes been studied

---

in tunneling systems (Josephson junctions) but critical phenomena, non-equilibrium phenomena, quasi-phenomenological effects, and numerous perturbations and parameter variations have been added to these experimental studies. Unfortunately, there has been slow transfer of this research knowledge to applications which might be useful to a more general community than research physicists. Fabrication of reliable Josephson devices (here referred to as all devices using pair electron processes) has been difficult, with only two <u>commercial</u> manufacturers emerging in the Josephson device area. However, these superconducting device manufacturers' markets and applications areas are highly limited. It has been only recently that enough of a marketplace has been established for Josephson devices even to allow these companies a normal return on their investment.

A contrast to the infant state of commercial Josephson devices is the solid state electronics industry. The initial development of semiconducting devices was similar to that of Josephson devices, but it has grown to an enormous and complex field. The major reason for this rapid growth was the competitive marketplace created by the demand for electronic devices. There is also a class of other devices using either superconductivity and/or semiconductor physics (e.g., super Schottky) or low temperature physics in the solid state (e.g., germanium detectors), which can be considered along with Josephson devices.

This paper reviews briefly the present marketplace in electronic devices to determine where Josephson devices are competitive. Further, this paper evaluates the marketplace for Josephson devices and gives an indication of some of the requirements placed on commercial manufacturing It shows that certain factors, that are not generally related to the inherent physical processes of the device, govern a significant portion of the effort in marketing electronic devices. The argument is that in order to make Josephson devices competitive with semiconductor devices, larger funding is necessary in a non-captive form.* This paper is intended as a means of stimulation to the community and all factual arguments are meant only to be concerned with rough order of magnitude values.

---

*A recent survey of the Superconductivity Industry is available from Business Community Co., Inc., Stamford, Connecticut; #E-032, for $625.

Where Do Josephson Devices Belong?

Before one can evaluate the market, one has to evaluate the useful applications of Josephson devices. A good starting point is a review of some of the more prominent and successful areas in which Josephson devices have been used:

- Low-noise devices: para-amps, mixers, detectors
- Sensor devices: magnetometers, voltmeters, galvometers
- Wide band – wide dynamic range devices: attenuators, comparators, A/D convertors
- Standard measurement devices: frequency standards, voltage standards
- Communications devices: receivers, cavity tuners, oscillators, etc.
- Computer devices: logic elements, memory cells.

It is useful to compare these applications with the present semiconductor market, where most solid-state electronic devices are the primary alternative. The general applications market for solid-state electronic devices falls into a few major areas, based on volume.

A. Standard Specifications Market

    1. Large Volume: a) Computer devices

                        b) Consumer devices

    2. Low Volume: a) Discrete devices

                        b) Low-noise devices.

                        c) Low-power devices

                        d) High-power devices

                        e) High-frequency devices.

B. Military Specifications Market — Low to intermediate volume

- High reliability requirements
- Power, weight, space requirements
- Environmental requirements
- Relaxed economic requirements

Josephson devices are useful in some of these areas, but they are not always competitive from a cost vs. performance standpoint. An examination of the large volume standard market suggests that there is a place for Josephson devices in the computer segment. However, for consumer applications, the severe environment requirements of Josephson devices rule out their use.

In the low volume market segment, there are a number of areas where Josephson devices can compete and, in some cases, be superior. However, these areas of applications are generally tied to a particular system. An example of this sub-component application is the need for a very low noise detector in a radar system, or a communications amplifier operating at frequencies in excess of present devices. Generally, the Josephson device would be a small part of an overall system, and would most likely be hand-tailored for each application. It is unlikely that Josephson devices would ever capture a significant share of even the low volume market.

Finally, there is the military specifications market. In some of these applications, cost, environmental considerations and other factors that are key to commercial sales do not apply. This is because military and security needs are placed above other considerations. In such cases, government-funded research programs would most likely develop specialized Josephson devices whose primary application would be as part of a larger system.

Thus, outside of specialized laboratory instruments, military applications, or low volume sub-component markets, Josephson devices will most likely be competitive only in the computer device area.

In support of this thesis, an example of a non-competitive application is the development of a Josephson frequency standard. After all the research and development, it is conceivable a company could find a market for ten units, at a sales price of $10K. However, a "booming" market in this non-competitive applications area would arise if, for example, the military decided to use this frequency standard at key facilities. Such a purchase might involve 500 units. This would create revenues of $5M, which compared to present Josephson device markets would be enormous. However, compared to the sales of virtually any type of semiconductor memory chip, this volume is insignificant. If two companies decided to market such a frequency standard, most likely the competition would bankrupt one of the companies. If a large company, like TRW or TI or Hughes, decided that it needed a Josephson-device-oriented radar front end, or a magnetometer sensor, the company would hire the needed specialist, couple him with its engineering staff, and incorporate the Josephson device into the overall system. It is unlikely that it would go out of house to develop or purchase any integral part of a large system that could not be second-sourced.

4

Computer Device Applications

The growth of computer usage has been enormous, exceeding all expectations. Not only are main frame computers being used for complex calculations, but the mini and micro computer market has made possible the use of dedicated computers for performing singular tasks. Table 1 shows some examples of the market variety and revenues. The data processing area is expected to double in dollar volume every five years through 1990.[1] Total user spending will rise to 13% of the GNP or $1,253 per capita (an increase of a factor of 10). Table 2 shows that by 1990, one in five workers will be using data processing skills and six out of ten will be depending on such skills. A recent decline in the ratio of government computers to total computers in the U.S. indicates that the large computer usage is expanding into commercial sectors. An example of these changing markets is the increasing use of computers in electronic banking. A Japanese banking system contains 8 main frame computers, 700 minis, and over 4000 computer terminals.[11]

Semiconductor Devices

In order to assess the potential utility of Josephson devices in the computer market, the technology of memory devices will be considered. In this discussion, only order of magnitude results are of interest. Consequently, memory and logic elements are used somewhat interchangably. Logic elements in computers can be thought of as a number of single unit devices with generally up to 8 devices to make one logic element in a computer. Thus, a rough rule of thumb is that a single device time of 10 ps would result in access or operation time of 8 times as much or 80 ps.[2] Since present main frame semiconductor computers are operating at logic cycle times of 5 ns (Amdahl 470/V7), their inherent device speeds (propagation delay) are on the order of 600 ps. Another factor in computers is the relation of the logic device or memory access time to the overall system time. About one third of the total access time is related to the device speed, and two thirds to the operating system, including hardware. Microcoding can reduce system time only by about 10%. While attempts

5

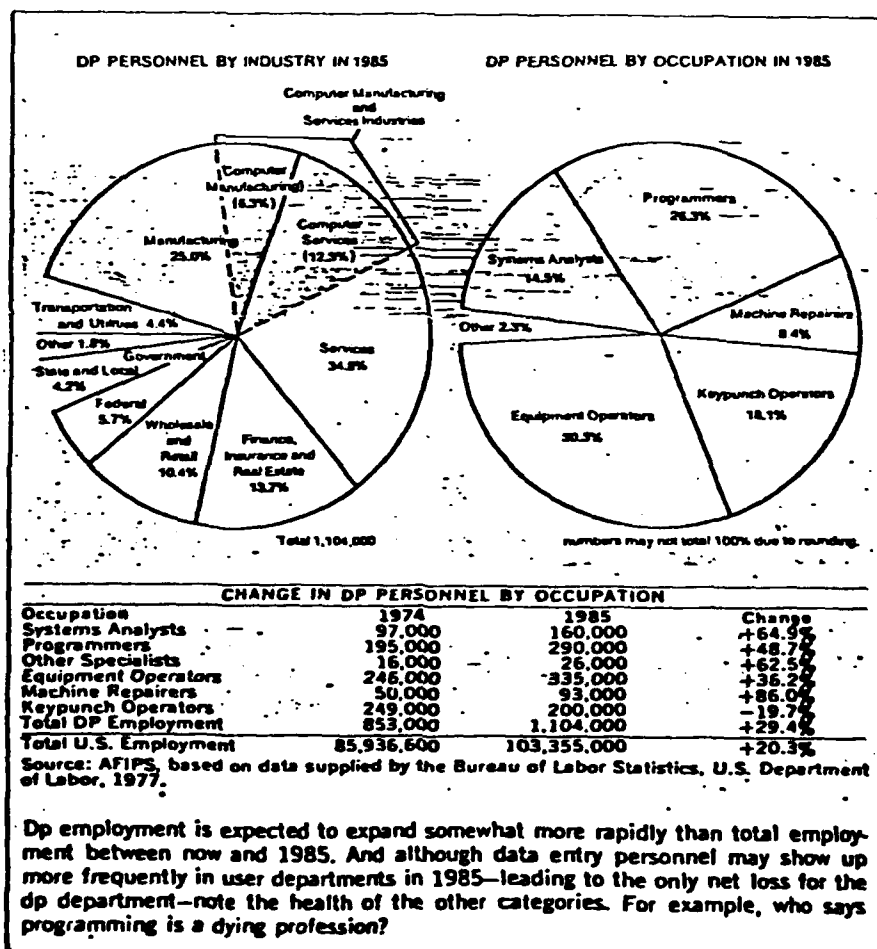## TABLE 1. CURRENT AND PROJECTED COMPUTER REVENUES GROUPED BY USAGE AREA [1]

WORLD REVENUES FOR U.S. FIRMS

	1971 ($ millions in 1971 dollars)			1976 ($ millions in 1976 dollars)			1981 ($ millions in 1976 dollars)
	U.S.	Overseas	World Total	U.S.	Overseas	World Total	World Total
EQUIPMENT							
General Purpose Computers	5,300	3,300	8,600	9,500	7,000	16,500	28,000
Mini & Dedicated Application Computers	250	60	310	1,200	800	2,000	7,000
Peripherals:							
Data Entry & Terminal Equip. from Mainframe Manufacturers	350	180	530	1,000	800	1,800	4,000
Data Entry & Terminal Equip. from Independent Suppliers	165	60	225	1,600	600	2,200	5,000
Machine Room Peripherals from Independent Suppliers	180	140	320	1,000	400	1,400	2,500
Leasing	600	70	670	1,000	100	1,100	1,500
Used Computer Sales	40	*	40	100	*	100	300
SERVICES							
Batch	950	110	1,060	1,700	200	1,900	2,400
On-Line	500	90	590	1,400	300	1,700	5,600
Software	750	40	790	1,100	500	1,600	5,000
Education	160	*	160	60	*	60	*
SUPPLIES	1,100	*	1,100	1,200	300	1,500	2,700
TOTALS	10,345	4,050	14,395	20,860	11,000	31,860	64,000

Source: AFIPS
*Negligible

The dollar value of computer shipments should approximately double in each five-year period, with the segment for minicomputers and dedicated application systems actually increasing much faster than that. (Note that some of the growth from 1971 to 1976 may be due to inflation.)

TABLE 2. INCREASES IN THE WORKING FORCE IN THE COMPUTER MARKET

DP PERSONNEL BY INDUSTRY IN 1985

DP PERSONNEL BY OCCUPATION IN 1985

CHANGE IN DP PERSONNEL BY OCCUPATION			
Occupation	1974	1985	Change
Systems Analysts	97,000	160,000	+64.9%
Programmers	195,000	290,000	+48.7%
Other Specialists	16,000	26,000	+62.5%
Equipment Operators	246,000	335,000	+36.2%
Machine Repairers	50,000	93,000	+86.0%
Keypunch Operators	249,000	200,000	-19.7%
Total DP Employment	853,000	1,104,000	+29.4%
Total U.S. Employment	85,936,600	103,355,000	+20.3%

Source: AFIPS, based on data supplied by the Bureau of Labor Statistics, U.S. Department of Labor, 1977.

Dp employment is expected to expand somewhat more rapidly than total employment between now and 1985. And although data entry personnel may show up more frequently in user departments in 1985—leading to the only net loss for the dp department—note the health of the other categories. For example, who says programming is a dying profession?

with parallel processing have been made (ILLIAC IV),[3] the general
computer industry may not see significant changes in system operations.
Consequently, significant (orders of magnitude) device speed reductions
are necessary to impact the overall logic or access time.

Another consideration in computer fabrication is the size of inherent
device elements and, for small size elements, the power dissipated per
device. The product of the logic device switching time and the power used
per gate is an energy quantity. For the most competitive semiconducting
device technology (I^2L in LSI),[2] the energy per gate is less than 10^{-12} J.
The power per gate is on the order of 200 μ watts with a switching speed of
a few ns. Lower power devices (CMOS) require longer switching times.
Faster devices (ECL) require more power. The area for such devices is on
the order of 4×10^{-5} cm^2/gate. This can be translated into a masking
technology of 60 μm/8 lines or a resolution of 8 μm (assuming an 8 line
by 8 line device). Standard photographic device fabrication techniques
easily can handle such resolution.[4] There exists a potential for using
x-ray lithography, to reduce device sizes, but such fabrication is quite
costly, is not expected to be in production until 1984, and only offers
a reduced fabrication resolution to 1/2 μm.[4] Reducing an I^2L device area
by a factor of 10^2 $((4\ \mu m/\frac{1}{2}\ \mu m)^2)$, would have the advantage of more devices
per chip, but also would increase the power dissipation per unit area by a
factor of 10^2 (assuming 10^2 more devices per unit area). Present values
of 5 μ watts/cm^2 would increase to 500 μ watts/cm^2, which is not acceptable
under normal device cooling methods.

Josephson Devices

Because the Josephson device operates with an energy gap 10^{-3}
times less than semiconductor devices, there is a potential for a computer
of the same size and power built with Josephson devices to have orders of
magnitude more capability. Flux motion devices have even lower power
requirements. However, only in satellites or special purpose installations
are such requirements necessary. An example is a computer used in an ICBM
defense system, to calculate trajectories in a minimal time, regardless of
cost. Such a system would be made as small as possible to reduce transit time

in calculations. Faster, larger, high density computers may be of major benefit to the areas of optical signal processing (10^{10} bits per picture),[5] weather prediction, and large scale simulators. An investment of $10M to simulate the operation of a $200M wind tunnel is an example of such large-scale simulations.

Josephson devices have been compared to semiconductor devices in numerous publications (see Reference 5). The energy per gate is on the order of 10^{-18} J for the flux shuttle, and it is higher for other superconducting devices (cryotron 10^{-15} J, JJ 10^{-15} J).[6] It was pointed out earlier that the device fabrication technology allows a reduction in area of present devices of up to a factor of 10^2. Since the same technology will limit Josephson devices, one can only expect a maximum reduction in computer size of the same factor. Power dissipation is not a problem at these lower superconducting energy levels.- However, if new cooling methods reduce a semiconductor device's power dissipation (such as a low temperature germanium device), this advantage is lost.

The Relationship Between Technology and Profit

To assess the commercial potential for a Josephson computer, the costs of fabrication have to be related to the benefits of new fabrication methods and to the time involved in establishing those methods in a production mode. Figure 1 displays two curves on separate axes in a 3-D plot (on this plot a device $\sim$ 10 bits of memory). The first curve is the time involved in establishing a higher density chip (devices/chip vs. development time). Presently, VLSI technology offers increases in devices per chip of factor of 5, but the development cost for such chips may be factors of 25. Eventually, such a curve has to break out into a non cost-effective technology. Note that yield in chip production goes inversely with fabrication difficulty. The other curve plotted relates the chip device density to the actual chip cost. Both these curves are using actual 1977 cost and technology time development data. Regions of fast slope on the devices/chip vs. chip cost indicate a lower cost/bit (LSI). Regions of slow slope indicate a high cost/bit. Eventually this curve will also break out into a non cost-effective region. Because the curve reflects present products sold by profit making

FIGURE 1. PROFIT MOTIVATION IN DEVICE TECHNOLOGY
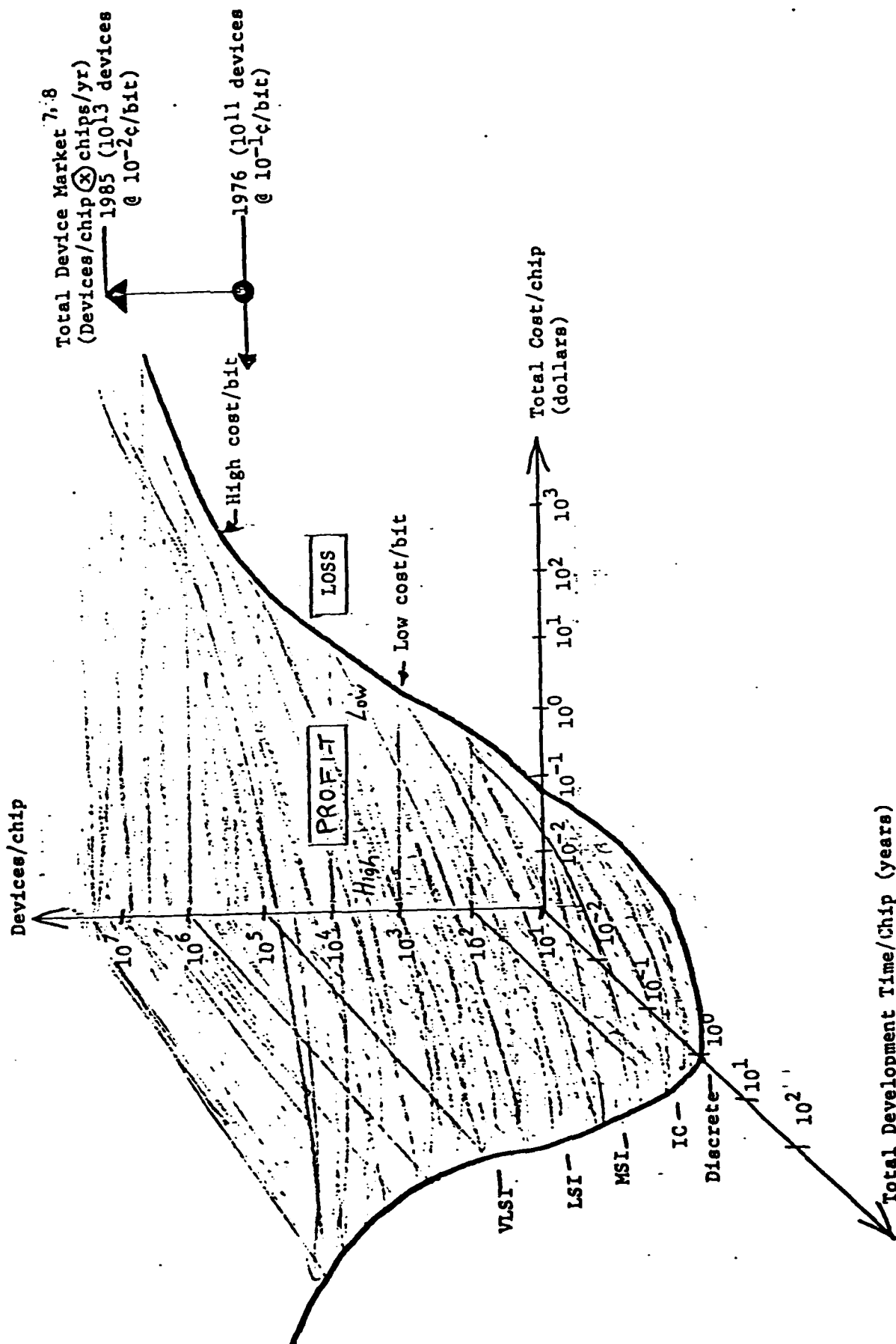
companies, it is assumed that more expensive chips with the same device/chip, would be a loss region for these companies. Consequently, a region of profit can be drawn between the two axes, to show how fabrication technology has to consider profit motivation. Higher profits will be obtained from technologies closer to the origin of Figure 1. In contrast to this plot, the cost and number of expected devices should decrease by 10 in cost/bit and increase by 10^2 in total devices in the 1985 market. The expected growth in bits per chip by 1985 is to a value on the order of 10^6 (Reference 3). The number of devices per chip (logic circuits) is expected to grow to 10^5. This growth will be moving in from the limits of the Figure 1 curve.

A direct comparison of all memory devices is shown in Figure 2. This figure also shows some additional large memories that are available off-the-shelf. The actual total size/bit, power, price, and speed is indicated. The access time of Josephson devices is also plotted, with no cost/bit information. It is obvious that although Josephson devices are not yet in production, they are technologically competitive. If the price/bit for Josephson devices can be reduced, by a production date of 1990, to a value lower than 10^{-2}¢/bit, they will be competitive. This would be equal to the projected semiconductor capabilities. This reasoning also can be applied to logic devices. However, if the price of Josephson devices is not reduced to lower than that value or if speeds are not significantly improved, they will only be used in special-purpose applications, because the competitive edge is not significant. In the next section, some factors relating to reducing such costs are discussed.

Device Research Costs

Figure 3 shows a typical development schedule for a single product line semiconductor device. This assumes no existing established practices. An example is ion-implantation or laser annealing in silicon. Generally, the first profits are not realized until many years after initial concept. Most of the costs are in labor. The final production yield dramatically affects the date and level of profits. For contrast, a similar projected development curve for the Josephson computer is inserted into Figure 3.

10

FIGURE 2. PRESENT MEMORY DEVICE TECHNOLOGY
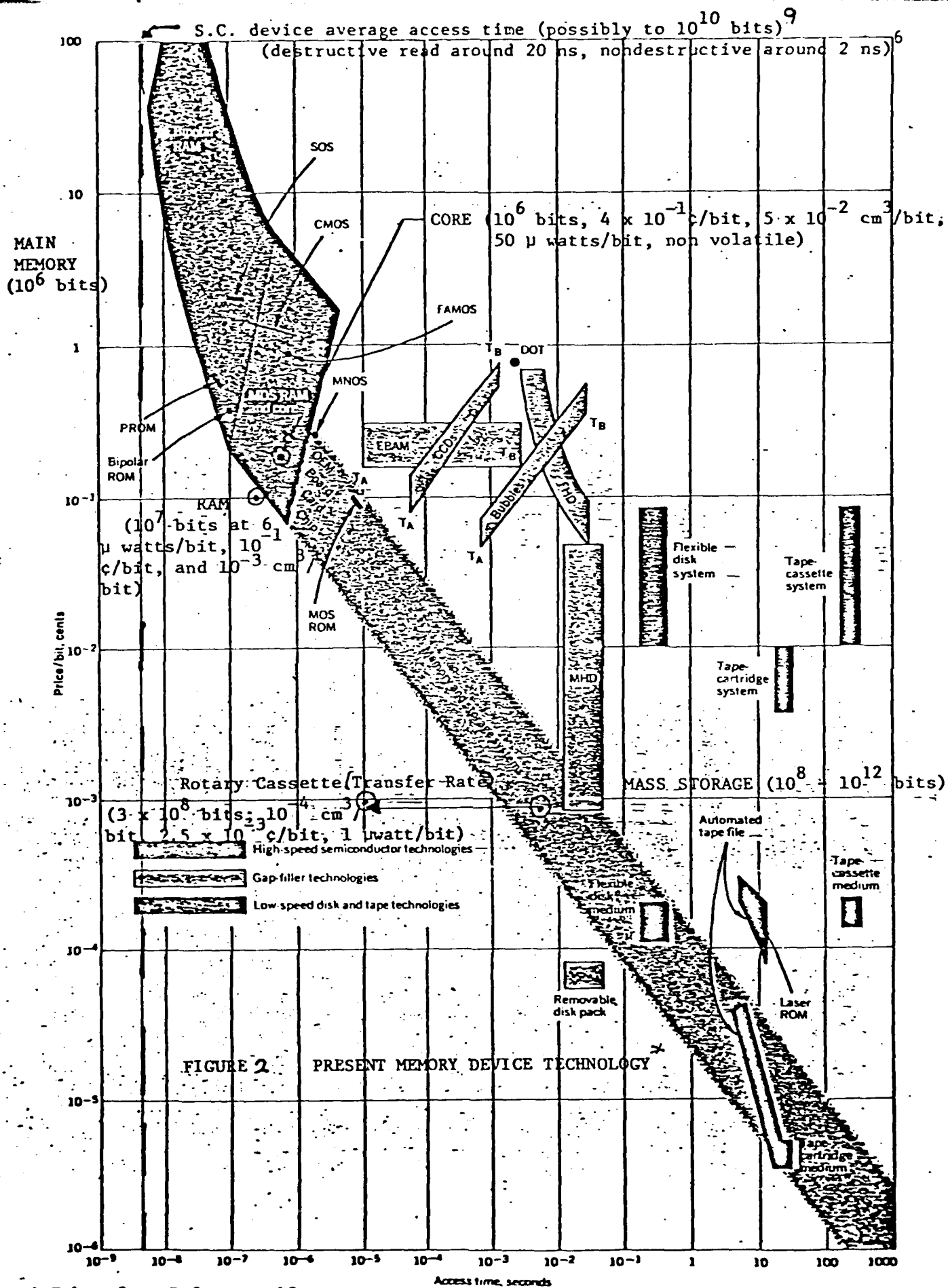
* Taken from Reference 13

11

FIGURE 3. DEVELOPMENT SCHEDULE FOR SINGLE SEMICONDUCTOR PRODUCT LINE VS. S.C. PRODUCT LINE
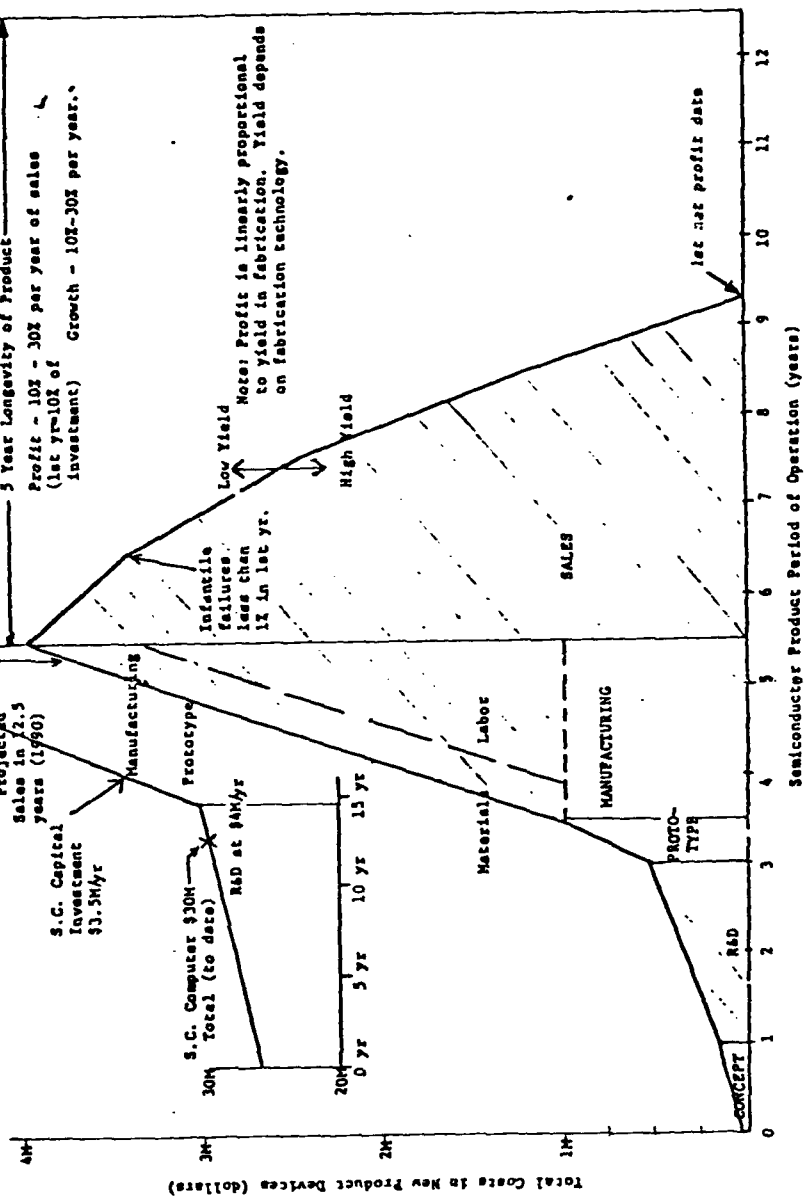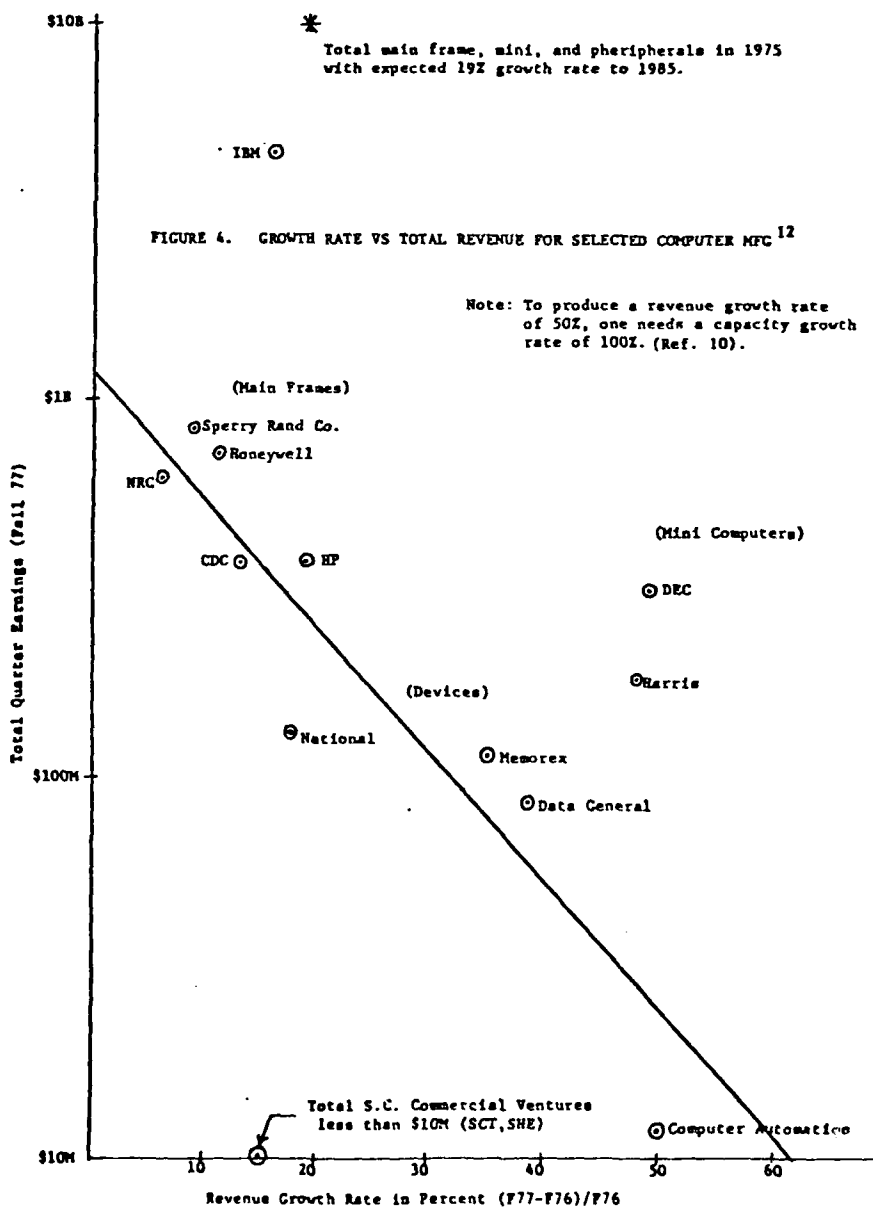
In general, most of these numbers are speculations made by the author.
If this curve is correct, it projects the Josephson devices to have a
development schedule five times longer and a development cost 10 times larger.
Surprisingly, this results in almost the same cost per year as in semiconductor
development. However, it predicts an initial sales date of 1990, assuming
that manufacturing starts in the next few years. Assuming that a manufacturing
investment of ten times that rate could be provided by IBM, increased
investment may not necessarily accelerate the first sales date.

The conclusion of this analysis is that Josephson device computers
can be on the marketplace by 1990, they can be technologically competitive,
but they may not be competitive from a cost standpoint. If they are not
cost competitive, they will fall into a special purpose category, useful
for only a few federal clients.

Who Can Afford to Develop Josephson Devices?

In an attempt to market Josephson devices in a competitive framework
by 1990, it is important to understand the capital that is necessary to
achieve such a goal. Figure 4 is a plot of some of the major computer
company's Fall '77 quarterly revenues vs. their growth rate over the previous
year. The main frame companies are larger and more conservative growth
companies. The minicomputers are faster growing, but smaller revenue
companies. It is noted that to achieve a growth rate of even 16% requires
a capacity growth of 32%. There are two companies that fall off the linear
relationship of Figure 4. They are IBM and DEC. Both companies established
computer markets and have enormous relative revenues. In order to compete,
other companies have had to reduce prices and experience rapid growth to
match the previous company's lead time. That rapid growth is a sign of
a competitive market. Also plotted in Figure 4 is the total estimated S.C.
commercial revenues for 1977. The actual value is most likely 10^3 times
below companies like IBM. It is obvious from the previous discussions that
in order to get to the competitive market in 1990, investments of $4M/yr
are needed. Such monies will not come from present, or even new, commercial
S.C. companies. However, it is quite easy for larger companies, with

$10B

Total main frame, mini, and pheripherals in 1975
with expected 19% growth rate to 1985.

IBM ⊙

FIGURE 4.   GROWTH RATE VS TOTAL REVENUE FOR SELECTED COMPUTER MFG [12]

Note: To produce a revenue growth rate
of 50%, one needs a capacity growth
rate of 100%. (Ref. 10).

$1B

(Main Frames)

⊙Sperry Rand Co.

⊙Honeywell

NRC⊙

(Mini Computers)

CDC ⊙   ⊙ HP

⊙ DEC

(Devices)

⊙Harris

⊙National

⊙Memorex

$100M

⊙Data General

Total Quarter Earnings (Fall 77)

Total S.C. Commercial Ventures
less than $10M (SCT,SHE)

⊙Computer Automatico

$10M

10   20   30   40   50   60

Revenue Growth Rate in Percent (F77-F76)/F76

14

enormous revenue, to invest at least at that level. Possibly ten times that rate ($40M/yr) could be afforded, but this would become 1% of some of the larger computer companies revenues (4 x $800M/yr), which is a sizeable portion of total expended research funds. Consequently, the present computer industry is one of the few places that is likely to invest in bringing Josephson device computers to maturity. However, such investments would have to be significant and have to be profit motivated. If these investments do not happen, then without competition, the single manufacturer of a low temperature (Josephson) computer (IBM) may provide a market only to special federal programs. In the conclusion, some means for altering this course are discussed.

Conclusion (Making the Josephson-Device Computer Competitive)

The author argues that in order to impact the future demands for computers, a Josephson computer will have to be competitive in not only technology but also in cost. If it is not, most likely the GaAs or other silicon technologies will surpass any technology benefits that might exist in the 1990s from a Josephson computer. Because of the system overhead, inherent device speeds do not directly control logic access times. The present semiconductor time delays of 600 ps will most likely be reduced in production systems, by the year 1990, to 300 ps, and to 100 ps, by the year 2000. Another cost factor that will influence a superconducting computer is the refrigeration cost. Present system cost for room temperature cooling can be as much as 5% of the overall computer cost.

What is needed to stimulate Josephson device computer development is many research groups with rapid interchange in a competitive atmosphere. An example of this in the semiconductor area is that SONY is planning to set up a research lab in "silicon valley" (Santa Clara, California) to be in a high technology area. However, SONY's manufacturing will remain in Japan. Josephson device research groups can only partially be set up by the Federal Government funding agencies. Because of unfulfilled low temperature device promises, there is little funding presently in low temperature research and large increases are not expected. This becomes a self-annihilating process. When, because of limited progress, little research is funded, the lack of funding leads to less research progress.

What is needed is for the large revenue computer companies to develop in-house programs in low temperature devices. But it is unlikely any of these companies would start at a $3M/yr level. A more believable route would be for new EE graduates to have a larger education in applied low-temperature device technology. Such graduate programs, possibly funded by the Federal Government, would strengthen the tie between universities and industry. Josephson devices could be treated as simple non-linear elements. Super-Schottky or low temperature Ge or Si devices may also be treated as simple non-linear elements. Unless the orientation of research shifts from the physicist to the design engineer, cost comparative decisions that will get the Josephson device computer to the competitive marketplace will not be made. Those decisions are made in the photolithographic room of an LSI manufacturer, not in the university research lab. The goal of a Josephson computer has to be to have a device time of 100 ps, an energy product of 10^{-2} pico J and a cost lower than 10^{-2} ¢/bit by the year 1990. The device size is not really necessarily important because it will be limited by fabrication technology. Through a competitive research program, originating in the present computer manufacturing companies, such goals may be reached.

References

1. P. M. McCarter, "Where is the Industry Going," Datamation, February 1978, p. 99.

2. P.W.J. Verhofstadt, "Evaluation of Technology Options for LSI Processing Elements," Proceedings of the IEEE, June 1976, p. 842.

3. H. Falk, "Reaching for a Gigaflop," IEEE Spectrum, October 1976, p. 65.

4. E. A. Torrero, "Solid State Devices," IEEE Spectrum, January 1977, p. 48.

5. R. W. Keyes, "Physical Limits in Digital Electronics," Proceedings of the IEEE, May 1975, p. 740.

6. H. H. Zappe, "Josephson Quantum Interference Computer Devices," IEEE Transactions on Magnetics, MAG-13, January 1977, p. 41.

7. N. Lindgren, "Semiconductors Face the 1980's," IEEE Spectrum, October 1977, p. 42.

8. R. Allen, "Semiconductor Memories," IEEE Spectrum, August 1975, p. 40.

9. R. A. Shaffer, "IBM Announces a Major Breakthrough in Solving Heat Problem in Computers," The Wall Street Journal, February 16, 1978, p. 36.

10. S. T. McClellan, "Will Success Spoil the Minicomputer Industry," Mini-Microsystems, May 1977, p. 30.

11. Y. Abe, "A Japanese On-Line Banking System," Datamation, September 1977, p. 89.

12. Mini-Micro Systems, January 1978; February 1978.

13. G. C. Feth, "Memories: Smaller, Faster and Cheaper," IEEE Spectrum, June 1976, p. 37.